

ALDRICHIMICA ACTA



Accelerating the Discovery of Next-Generation Small-Molecule Protein Degraders

Coumarin-Based Hybrids as Fluorescent Probes for Highly Selective Chemosensing and Biological Target Imaging

**MERCK**

DEAR READER:

¹ The New York Times, Nov. 26, 2018

² Vox, Jan. 22, 2019

Over the past few months, alarmist headlines such as **“Chinese Scientist Claims to Use CRISPR to Make First Genetically Edited Babies¹”** and **“Is the CRISPR baby controversy the start of a terrifying new chapter in gene editing?²”** have appeared with some frequency in mainstream media worldwide.

As scientists, researchers, and innovators of gene-editing technology, we have a responsibility to seek out the best minds in bioethics to educate us, guide us and help us navigate this uncharted territory.

This is why Merck KGaA, Darmstadt, Germany established a **Bioethics Advisory Panel**, which includes leading external experts representing law, ethics, medicine and science from the US, Europe, Africa and Asia. The panel meets annually to explore, discuss and provide a wider worldview of the impact of our technologies, research and therapies on human health, agriculture and even all living beings. Thus far, with the panel’s help, we have published clear guidelines for our business on fertility treatments, stem cell research, clinical trials and off-label use, among other important topics.

Most recently, in collaboration with our Gene Editing & Novel Modalities team, the panel provided a clear statement of our **position** on gene editing. This led to a published paper, **Ethical Considerations in the Manufacture, Sale and Distribution of Genome Editing Technologies**, in *The American Journal of Bioethics*.

As we continue to explore and innovate in this exciting area of science, we will continue to ask the tough questions and seek the answers necessary to advance gene-editing ethically and responsibly for our customers and mankind.

Sincerely yours,

Udit Batra, Ph.D.
CEO, Life Science
Member of the Executive Board,
Merck KGaA, Darmstadt,
Germany

Merck KGaA
Frankfurter Strasse 250
64293 Darmstadt, Germany
Phone +49 6151 72 0

To Place Orders / Customer Service

Contact your local office or visit
SigmaAldrich.com/order

Technical Service

Contact your local office or visit
SigmaAldrich.com/techinfo

General Correspondence

Editor: Sharbil J. Firsan, Ph.D.
Sharbil.Firsan@milliporesigma.com

Subscriptions

Request your FREE subscription to the
Aldrichimica Acta at SigmaAldrich.com/acta

The entire *Aldrichimica Acta* archive is available
at SigmaAldrich.com/acta

Aldrichimica Acta (ISSN 0002-5100) is a
publication of Merck KGaA.

Copyright © 2019 Merck KGaA, Darmstadt,
Germany and/or its affiliates. All Rights
Reserved. Merck, the vibrant M and Sigma-
Aldrich are trademarks of Merck KGaA,
Darmstadt, Germany or its affiliates. All
other trademarks are the property of their
respective owners. Detailed information on
trademarks is available via publicly accessible
resources. Purchaser must determine the
suitability of the products for their particular
use. Additional terms and conditions may
apply. Please see product information on the
Sigma-Aldrich website at SigmaAldrich.com
and/or on the reverse side of the invoice or
packing slip.

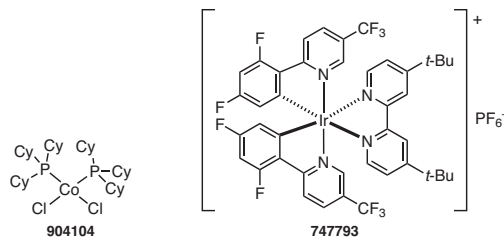


"PLEASE BOTHER US."

Dear Fellow Chemists,

Professor Tomislav Rovis of the Department of Chemistry at Columbia University kindly suggested that we offer dichlorobis(tricyclohexylphosphine)cobalt(II) (**904104**), which, in combination with the photocatalyst ($\text{Ir}[\text{dF}(\text{CF}_3)\text{ppy}]_2(\text{dtbpy})\text{PF}_6$) (**747793**), enables the facile formation of arenes at room temperature by a spatially and temporally resolved $[2 + 2]$ alkyne cycloaddition using visible light as an external stimulus.

(1) Ruhl, K. E.; Rovis, T. *J. Am. Chem. Soc.* **2016**, *138*, 15527. (2) Ravetz, B. D.; Ruhl, K. E.; Rovis, T. *ACS Catal.* **2018**, *8*, 5323. (3) Ravetz, B. D.; Wang, J. Y.; Ruhl, K. E.; Rovis, T. *ACS Catal.* **2019**, *9*, 200.



| | | |
|---------------|---|------------------|
| 904104 | Dichlorobis(tricyclohexylphosphine)cobalt(II) | 250 mg 100 mg |
| 747793 | $[\text{Ir}[\text{dF}(\text{CF}_3)\text{ppy}]_2(\text{dtbbpy})]\text{PF}_6$ | 100 mg 1 g |

We welcome your product ideas. Do you need a product that is not featured on our website? Ask us! For more than 60 years, your research needs and suggestions have shaped our product offering. Email your suggestion to techserv@sial.com.

Udit Batra, Ph.D.
CEO, Life Science

TABLE OF CONTENTS

Accelerating the Discovery of Next-Generation Small-Molecule Protein Degraders **35**

Sarah Schlesiger,* Momar Toure,* Kaelyn E. Wilke, and Bayard R. Huck, Merck KGaA,
Darmstadt, Germany

Coumarin-Based Hybrids as Fluorescent Probes for Highly Selective Chemosensing and
Biological Target Imaging **51**

Carla Santana Francisco, Thays Cardoso Valim, Álvaro Cunha Neto, and Valdemar Lacerda, Jr.,*
Federal University of Espírito Santo, Vitória, Brazil

ABOUT OUR COVER

The Square of Saint Mark's, Venice (oil on canvas, 114.6 x 153 cm) was painted in 1742/1744 by the renowned Venetian cityscape painter Giovanni Antonio Canal (1697–1768), better known as Canaletto. He apprenticed with his father and brother, painting scenes for the theater and, except for a decade-long stay in England, Canaletto spent all his life in Venice.

In his mid-twenties, Canaletto shifted to painting detailed and accurate scenes of daily life in his native Venice for foreign visitors (mainly English) as mementos of their visit. As a result, Canaletto became widely known and appreciated outside Italy, particularly in England, where many collectors of his paintings lived. While Canaletto also created compositions of scenes in Rome and London, and produced a number of fine etchings, he is best-known for his "vedute" of Venice and surrounding area.*

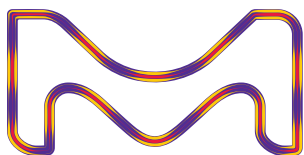
Canaletto's almost photographic rendering of the scene in this painting—with his meticulous depiction of the architecture, light effects, sky and clouds, and realistic colors—beautifully captures the atmosphere and vitality of the square and brings it to life. Were it not for the clothes, hats and sailing ships, one could mistake this scene as one happening now in Venice. Canaletto achieved considerable fame during his lifetime and influenced later generations of landscape artists in England and elsewhere. Of his many pupils, the best-known is his nephew, the accomplished landscape painter Bernardo Bellotto.*

A gift of Mrs. Barbara Hutton, National Gallery of Art, Washington, DC.

* To find out more about Canaletto, his many paintings of Venetian scenes, and his influence, visit
SigmaAldrich.com/Acta



Detail from *The Square of Saint Mark's, Venice*.
Photo courtesy National Gallery of Art,
Washington, DC.



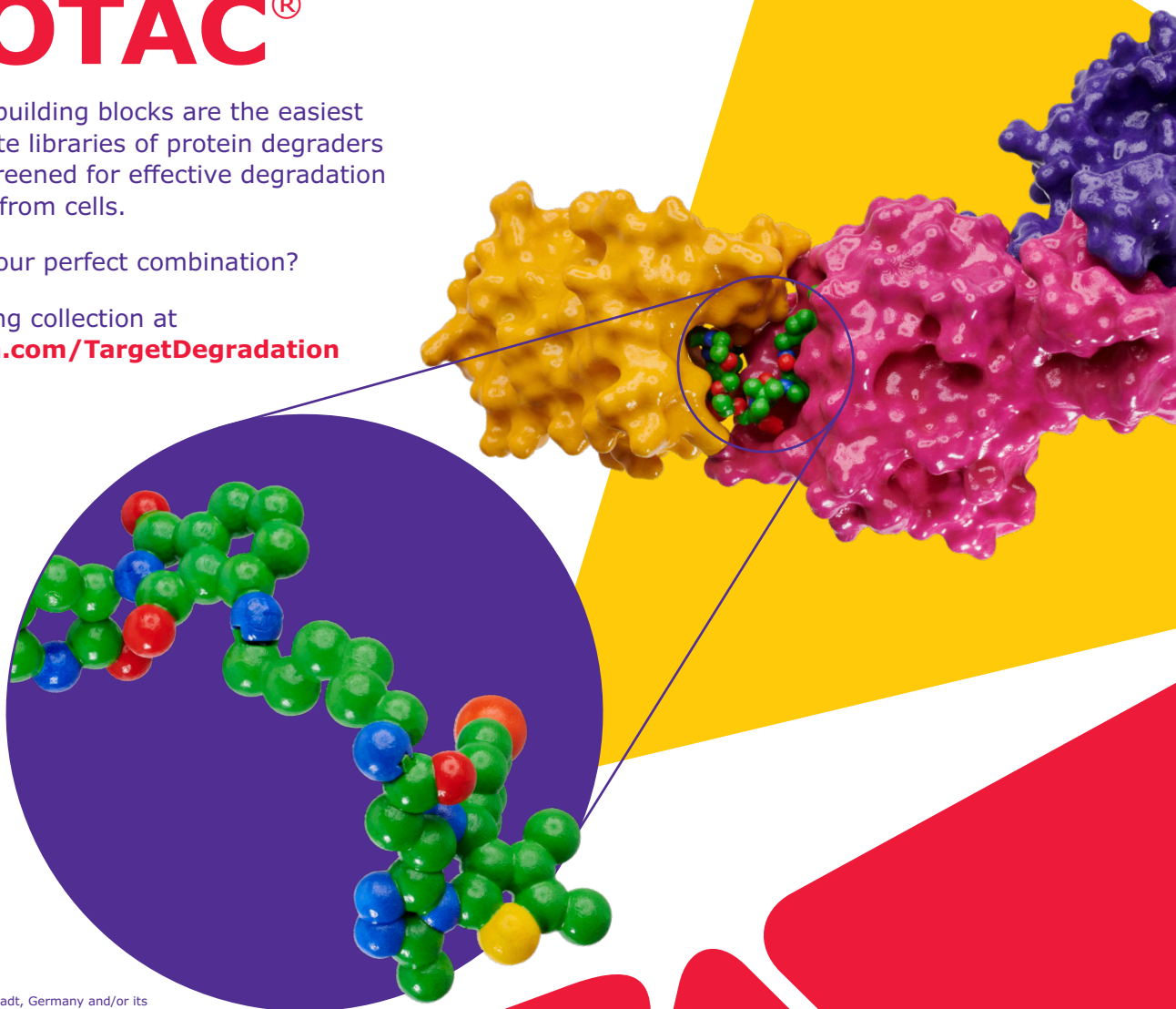
MERCK

DESIGN THE PERFECT PROTAC[®]

Our degrader building blocks are the easiest way to generate libraries of protein degraders that can be screened for effective degradation of your target from cells.

What will be your perfect combination?

See our growing collection at
SigmaAldrich.com/TargetDegradation



© 2020 Merck KGaA, Darmstadt, Germany and/or its affiliates. All Rights Reserved. Merck and the vibrant M are trademarks of Merck KGaA, Darmstadt, Germany or its affiliates. PROTAC[®] is a registered trademark of Arvinas Operations, Inc., and is used under license. All other trademarks are the property of their respective owners. Detailed information on trademarks is available via publicly accessible resources.

31262 04/2020

The life science
business of Merck
operates as
MilliporeSigma in the
U.S. and Canada.

Sigma-Aldrich[®]
Lab & Production Materials

Accelerating the Discovery of Next-Generation Small-Molecule Protein Degraders



Dr. S. Schlesiger



Dr. M. Toure



Dr. K. E. Wilke



Dr. B. R. Huck

Sarah Schlesiger,^{*a} Momar Toure,^{*b} Kaelyn E. Wilke,^c and Bayard R. Huck^b

^a Department of Medicinal Chemistry, Merck KGaA, Frankfurter Strasse 250, 64293 Darmstadt, Germany
Email: Sarah.Schlesiger@merckgroup.com

^b EMD Serono R&D Institute, Inc., 45A Middlesex Turnpike, Billerica, MA 01821, USA
Email: Momar.Toure@emdserono.com

^c Chemical Synthesis Department, MilliporeSigma, 6000 N. Teutonia Avenue, Milwaukee, WI 53209, USA

Keywords. proteolysis-targeting chimera; degronimid; degon; protein degraders; PROTAC®; Partial Degraders; SNIPER; drug discovery; undruggables.

Abstract. Currently, many pharma and biotech companies as well as academic laboratories are developing PROTAC programs to investigate whether induced protein degradation offers new insights into a protein's pharmacological utility and new treatment opportunities for their high-value therapeutic targets. Within this review, we aim to explain the complexities and empiricism inherent in designing proteolysis-targeting chimeras, which result in the synthesis of compound libraries for the discovery of lead molecules with degrader potential. Due to typically limited resources in exploratory projects or concept space, this required synthesis of large compound libraries to fully explore PROTAC options is a high barrier to overcome. Thus, we also comment on how to strategically choose which molecules to synthesize and how the use of commercial building blocks can accelerate the discovery of degraders. Additionally, we describe the available assays for profiling PROTACs.

Outline

1. Introduction
 - 1.1. State of the Art in Protein Degradation
 - 1.2. Recent Progress in the PROTAC Field

- 1.3. Linkers and Exit Vectors
2. PROTAC Library Design
3. Profiling of PROTAC Compounds
 - 3.1. Binding Confirmation
 - 3.2. Degradation Assay
 - 3.2.1. Choosing a Cell Line
 - 3.2.2. Effect of PROTAC Concentration on Assay
 - 3.2.3. Assay Time Points
 - 3.2.4. Assay Controls
 - 3.2.5. Protein Detection Methods
 - 3.3. Kinetic Profiling and MoA Studies of Degraders
4. Conclusion
5. References

1. Introduction

In the last decade, the development of **proteolysis-targeting chimeras** (PROTACs) has emerged as a new therapeutic modality.¹⁻³ PROTAC compounds are small, hetero-bifunctional molecules that target proteins for degradation by recruiting an E3 ligase in the vicinity of the protein of interest (POI). This proximity enables E3 ligase-mediated ubiquitination of the target protein followed by consecutive recognition and degradation by the proteasome. In this way, the PROTAC hijacks the native cellular degradation mechanism to selectively remove the POI from the cell (**Figure 1**, Part (a)).⁴ As a result,

PROTAC technology has a great potential as a new therapeutic approach for the treatment of cancer and other protein-related diseases, for which traditional drug discovery has not led to effective treatments. It is estimated that only a small portion (~10%) of the human proteome is accessible with contemporary inhibitor-based, small-molecule drug programs,^{5,6} and targeted protein degradation has the potential to significantly expand the modern medicinal chemistry druggable space.

The limitations of small-molecule, inhibitor-based pharmacology have strongly motivated the development and use of genetic techniques to successfully remove or decrease the expression of disease-causing proteins within the cell (Figure 1, Part (b)). RNAi,^{7,8} antisense oligonucleotides,^{9,10} and more recently CRISPR^{11–13} can be used “on demand” to control protein levels. These genetic strategies, however, suffer from several limitations^{14–17}—including the need for genetic manipulation, off-target issues, lack of cell permeability, and poor pharmacokinetics—thus making the translation of these technologies to the clinic highly challenging. Fortunately, PROTAC-mediated targeted protein degradation can overcome these challenges.^{18–23} A PROTAC molecule transiently interacts with a POI and E3 ligase prior to POI ubiquitination and degradation by the 26S proteasome, but the PROTAC is not degraded alongside the POI. Consequently, this degradation approach to drug discovery and development differs in two key ways from inhibitor-based pharmacology: (i) The cell needs to resynthesize the POI after treatment before protein function is restored, and (ii) in contrast to the “one drug, one target” model of inhibitor-based pharmacology, a PROTAC compound can be catalytic, with one degrader molecule transiently binding and removing multiple POIs. Thus, this approach offers several advantages over the traditional drug paradigm: (a) Abrogation of protein function can be accomplished at lower

drug concentrations due to the catalytic nature of the PROTAC. (b) Modulation of the POI function can be achieved with less exposure time of the drug due to POI removal. (c) Difficult-to-drug targets—such as transcription factors, regulatory/scaffolding proteins, and non-enzymatic proteins—can be targeted since binding at any protein surface is all that is required for modulation. (d) Additional feedback loops or significant scaffolding roles perpetuated by inhibitor-occupied proteins would be lost upon degradation (similarly to genetic knockdowns). (e) Finally, resistance by gene overamplification can be overcome once again due to the catalytic nature of the PROTAC agent.

ARV-110, an oral androgen receptor (AR) degrader, entered clinical trials in the first quarter of 2019 for the treatment of patients with metastatic, castration-resistant prostate cancer (mCRPC), and could demonstrate the technology’s therapeutic potential. Nonetheless, this novel technology has proven to be a valuable tool to study target engagement and validation. Moreover, since its discovery, many proteins—ranging from kinases to signaling proteins, cytosolic proteins, and membrane receptors—have been knocked out by degraders.

1.1. State of the Art in Protein Degradation

Almost 20 years ago, Sakamoto et al. reported that an I κ B α phosphopeptide inhibitor conjugated with ovalicin was able to recruit the E3 ligase SCF ^{β} -TRCP and successfully induce the degradation of the target protein methionine aminopeptidase-2 (MetAP-2).^{4b} While being the first PROTAC proof of concept, the peptide ligand used lacked cell permeability, which limited its therapeutic utility. The groups of Crews, Deshaies, and Kim followed this seminal study with extensive research on next-generation PROTAC degraders that possess better physicochemical properties.^{24–28} This effort led to the first cell-permeable PROTAC that targets

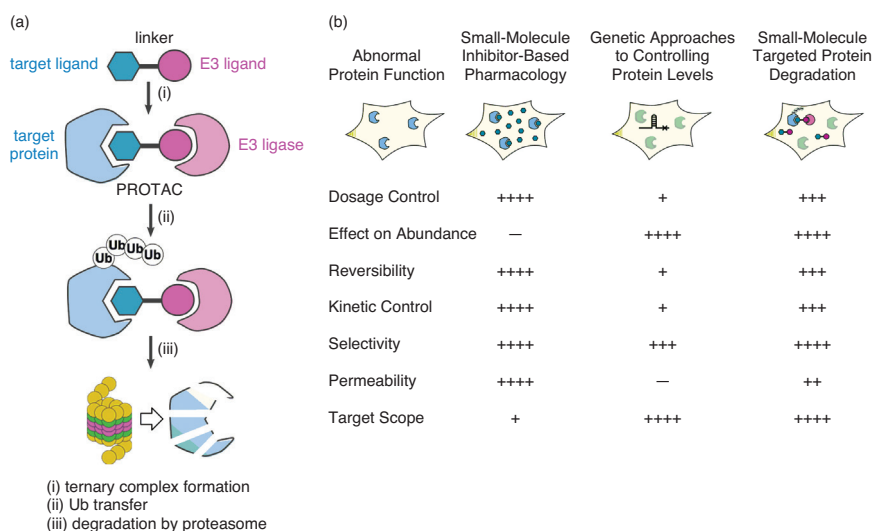


Figure 1. (a) Mechanism of Targeted Protein Degradation Mediated by PROTAC. (b) Comparison of Protein-Centric Drug Discovery Strategies (Small-Molecule Inhibitor-Based Pharmacology, Genetic Approaches to Control Protein Levels, and Small-Molecule Targeted Protein Degradation). (Ref. 4)

androgen and estrogen receptors, then the first in vivo PROTAC proof of principle, and ultimately to the future development of all small-molecule degraders.²⁹

Despite the impressive progress made beginning with the seminal, impermeable peptidic PROTAC to the subsequent demonstration of phosphoPROTAC-induced targeted protein degradation in vivo, the development of small-molecule degraders remained very limited. This was due to the unavailability of effective small-molecule E3 ligase ligands. The only known example was the nutlin/AR ligand that was reported by Crews and co-workers in 2008 for MDM2-mediated degradation of AR in prostate tumor cells (Figure 2).³⁰ Unfortunately, however, the nutlin/AR PROTAC was less effective than the early peptidic degrader. Two years later, Hashimoto's research team found that bestatin esters can effectively recruit the E3 ligase cIAP1 and successfully knockdown both target proteins and cIAP1 itself through autoubiquitination and degradation, resulting in cell toxicity.³¹ To address this challenge and develop small-molecule PROTAC hybrids with desirable physicochemical properties along with better potency, the laboratory of Crews designed and developed small-molecule ligands that potently bind to the primary HIF-binding site on the von Hippel-Lindau (VHL) E3 ubiquitin ligase.^{32,33} This ligand was further optimized by Ciulli's group to afford a series of potent VHL ligands.^{34,35} Other studies have revealed that thalidomide and its derivatives, lenalidomide and pomalidomide, bind to

the E3 ligase complex cereblon (CRBN) and induce proteasomal degradation of the transcription factors Ikaros (IKZF1) and Aiolos (IKZF3)—that being the mechanism of action of these important immunomodulator drugs in multiple myeloma.^{36–39} The availability of these ligands (Figure 3) for both VHL and CRBN E3 ligases accelerated the discovery—independently, by the research groups of Crews¹⁸, Ciulli,²⁰ and Bradner²¹—of multiple small-molecule PROTACs, including degraders that target members of the BET family, BRD4/3/2. For example, ARV-825 was found to induce nearly complete degradation of BRD4 at 10 nM.¹⁸ Bradner's team went further and showed that small-molecule PROTAC degraders are effective in vivo.²¹ In fact, 50 mg/kg (ip, qd) dBET1 treatment of a mouse model led to an impressive lymphoma tumor regression in 14 days. Interesting additional evidence of PROTAC-induced degradation was revealed with the hook effect, which describes the loss of efficacy at increasing PROTAC concentrations. Further insight about the PROTAC mechanism was gained when Ciulli's group solved the first co-crystal structure of a VHL PROTAC, MZ1, interacting with both the target protein BRD4 and the E3 ubiquitin ligase VHL at their interface.⁴⁰ This interaction between target, E3 ligase, and PROTAC is called the “ternary complex.” Notably, the protein–protein interaction created by this ternary complex illustrates the complexity of designing a PROTAC. The role of the ternary complex formation and the importance of that protein–protein interaction were investigated by Calabrese

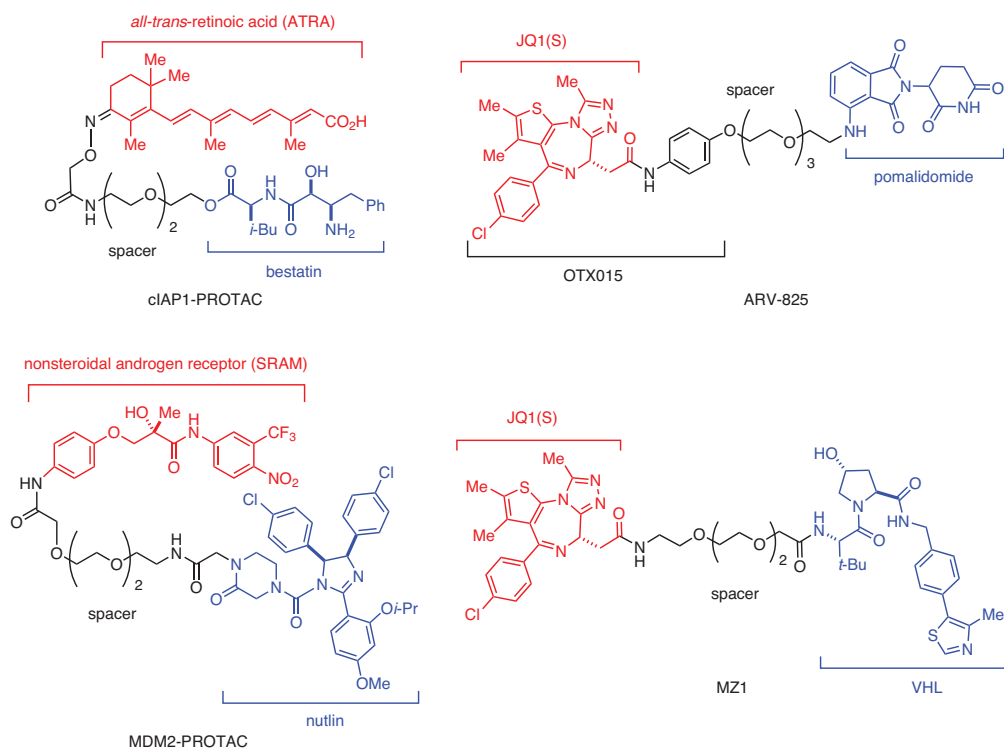


Figure 2. Structures of Selected PROTACs Derived from Popular E3 Ligase Ligands. (Ref. 18,20,21,30–40,47)

and co-workers.⁴¹ By developing PROTACs that target BTK, these authors found that the ability of a PROTAC to induce a stable ternary complex is necessary for degradation, but cooperativity was not a key factor. In contrast, thermodynamic entropy/enthalpy was found to be crucial in terms of degradation efficacy. Taken together, the ability of a given PROTAC to form a stable ternary complex might govern potency and selectivity. This hypothesis is in accord with recent work by Crews's group who found that a foretinib-based PROTAC that weakly binds to protein p38 α ($K_D \sim 11 \mu\text{M}$) was able to efficiently degrade p38 α with a half maximal degradatory concentration (D_{max}) of 210 nM.⁴² This very surprising finding of increased potency could raise questions of potential unexpected off-target degradation. Interestingly, Winter's and Bradner's groups reported that MI-389, a sunitinib-based PROTAC, failed to induce degradation of consensus targets including cKIT plus 40 other kinases.⁴³ Despite lack of target degradation, an off-target was identified. Comparative profiling via quantitative mass spectrometry of untreated proteomes and those treated with MI-389 demonstrated the sole degradation of the translation termination factor GSPT1 among 6490 proteins quantified, highlighting the power of quantitative proteomics to investigate off-target effects due to unintended E3 ligase modulation. Another very promising characteristic of PROTACs is the fact that they may provide unexpected selectivity. Many such examples are described in the kinase field, where PROTAC derivatives of very promiscuous kinase inhibitors such as TL12-186⁴⁴ and foretinib⁴³ yielded more selective kinase

degraders. For instance, the promiscuous diaminopyrimidine-based inhibitor TL12-186 binds over 100 known kinases; however, the PROTAC derivate of TL12-186 degraded only 28 kinases. This additional layer of selectivity can be rationalized by the requirement to produce a stable and productive ternary complex for the degradation to happen.⁴⁵ More recently, the promiscuous FLT-3 inhibitor quizartinib was conjugated with a VHL ligand, producing a more selective degrader. Additionally, FLT-3 PROTAC had acceptable pharmacokinetics (PK) with half maximal inhibitory concentration (IC_{50}) coverage after 20 hours (10 mg/kg, ip). A further pharmacodynamics (PD) study showed that PROTAC FLT-3 could induce the degradation of FLT-3 in vivo with a 30 mg/kg treatment (ip, qd).⁴⁶

1.2. Recent Progress in the PROTAC Field

A better understanding of the mechanism of action of PROTACs, along with more widely available E3 ligase ligands, accelerated the early proof of concept to a currently viable therapeutic approach with these molecules. Several therapeutically relevant proteins have been successfully degraded this way, either partially or near completely, and most of this work has been extensively reviewed.⁴⁷ Notably, a successful use of an MDM2 E3 ligase recruiting PROTAC with dual function (degrader/inhibitor) has been reported.⁴⁸ Nutlin-based PROTAC A1874 was able to degrade BRD4 and thus suppress oncogenic protein Myc expression by 85% relative to control. In addition, since nutlin itself is an MDM2 inhibitor, PROTAC A1874 also upregulated p53 via MDM2 inhibition. Furthermore, the loss of cell viability, when

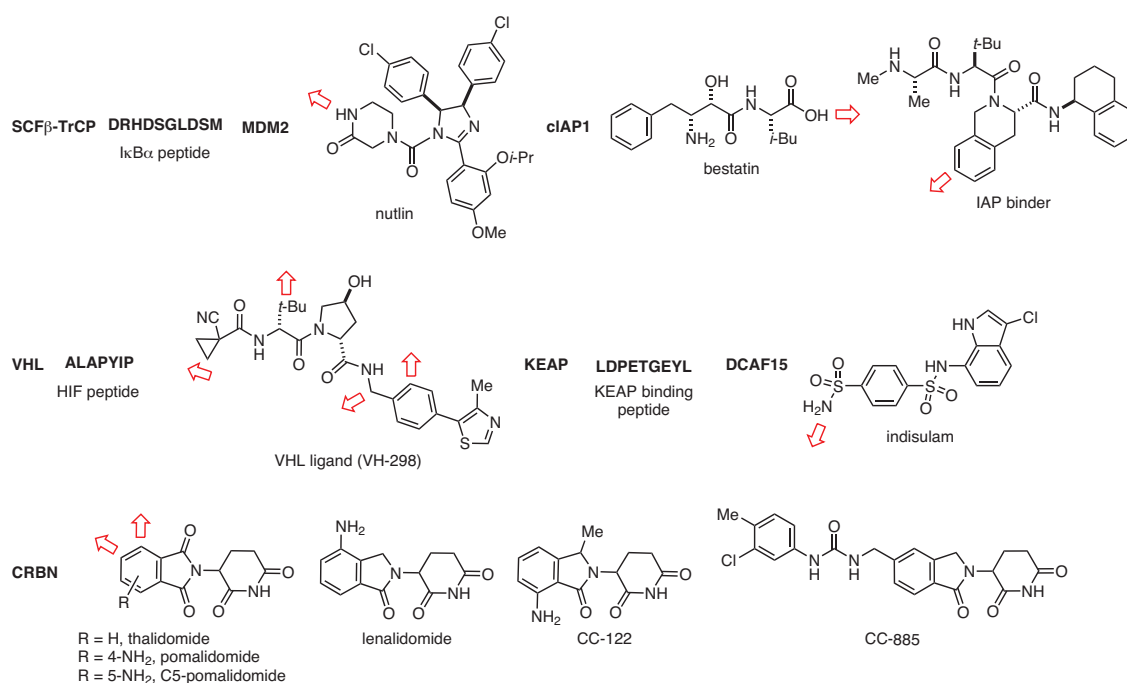


Figure 3. Applied E3 Ligases, Their Binders, and Their Exit Vectors.

different cell lines were treated with A1874, was confirmed to be superior to the sum of the effects of the MDM2 inhibitor idasanutlin alone and JQ1 alone.⁴⁸ Given the important roles of Myc and p53 in cancer (tumor suppressor regulation, DNA repair, cell cycle arrest, and apoptosis), this successful PROTAC with a dual function could offer more robust therapeutic effects. Very recently, PROTAC technology has been established as a valuable tool for intracellular target engagement validation in the absence of downstream molecular pharmacodynamic biomarkers in the case of the protein pirin.⁴⁹ The authors found that, not only did a pirin ligand based PROTAC degrade the target protein, it also competed with the original ligand to bind to pirin when co-incubated. Similarly, PROTACs were employed as potent and selective tools to study BCL6 biology. Scientists from AstraZeneca found, however, that neither BCL6 inhibitors nor BCL6 degraders could produce the expected phenotypic response when applied in DLBCL, therefore highlighting the challenges associated with small-molecule targeting of BCL6.⁵⁰ Targeted protein degradation was elegantly used to address the kinase-independent functions of Focal adhesion kinase (Fak), a protein possessing simultaneous kinase and scaffolding roles for several signaling proteins.⁵¹ In this effort, a defactinib derivative linked to a VHL ligand yielded PROTAC-3, a highly selective, low nanomolar-potency Fak degrader with a DC_{50} value of 3.0 nM as well as an excellent D_{max} of 99%. In addition, PROTAC-3 is five times more selective than the clinical candidate defactinib (Verastem VS-6063) since it binds only 20 kinases at 1 μ M. In a direct comparison between PROTAC-3 and defactinib, the authors found that PROTAC-3 outperformed defactinib in reducing Fak downstream target paxillin. Treatment with 50 nM of PROTAC-3 caused over 85% reduction of p-paxillin levels. In comparison, defactinib reduced p-paxillin levels by only 62% at 10 μ M. In addition, 50 nM PROTAC-3 treatment was found to impair cell migration and reduce cell wound healing by 53%. As expected, the Fak scaffolding role was overcome by targeting Fak for degradation with PROTAC, while the inhibitor failed. More recently, the oncogenic translation initiation factor protein eIF4E was targeted with a PROTAC. Through an impressive synthetic route, the authors generated a series of GMP lenalidomide-based PROTACs.⁵² Unfortunately, these molecules were not able to induce eIF4E proteasomal degradation. Whether this result is due to lack of cell permeability or available lysine for the ubiquitination step remains to be determined.

The first degrader targeting poly(ADP-ribose) polymerase-1 (PARP1), which plays crucial roles in DNA-damage signaling, was successfully developed by Rao's group.⁵³ Niraparib conjugated to a nutlin derivative yielded a degrader that led to selective and significant reduction in PARP1 levels enough to induce an enhanced apoptotic response in the MDA-MB-231 breast cancer cell line, resulting in the observed caspase-3 cleavage. A control experiment confirmed this hypothesis since niraparib or nutlin-3 alone and in combination failed to cause any detectable caspase-3 cleavage. In a recent study, Focal adhesion tyrosine kinase (PTK2) was degraded by hijacking E3 ligases. Scientists at Boehringer Ingelheim found that even though a series of

PROTACs potently and selectively caused PTK2 degradation with an average DC_{50} in the low nanomolar range, these molecules failed to affect proliferation of the tested cell lines in comparison to the PTK2 inhibitor BI-4464 alone.⁵⁴ This data suggests that PTK2 might not possess significant scaffolding roles or that its scaffolding function is not required for in vitro cell proliferation. A group of scientists from the University of Calgary reported that the "undruggable" antiapoptotic protein myeloid cell leukemia 1 (MCL1) could also be targeted for PROTAC-mediated degradation.⁵⁵ MCL1 is an ideal PROTAC target because it plays a role in complex protein-protein interactions (that promote cell survival) involving the pro-apoptotic factors Bim, Bak, and Bax. MCL1 inhibitor A-1210477 was coupled with thalidomide analogues for CRBN recruitment. After an extensive study with docking and linker exit vector variation, optimized PROTAC dMCL1-2 caused MCL1 reduction at 500 nM in HeLa cells. MCL1 degradation resulted in apoptosis at 250 and 500 nM after 24 hours of treatment, as revealed by Caspase-3 cleavage.⁵⁵ Since MCL1 possesses a rapid turnover rate, the authors confirmed that the observed MCL1 level reduction was indeed caused by PROTAC-mediated proteasomal degradation.⁵⁵ This innovative work once again highlights the potential of the PROTAC approach as an alternative way to target the so-called "undruggable" proteins. Another property underscoring the novelty of PROTACs is their catalytic, event-driven mechanism. The impact of the catalytic effect on PROTAC degradation profile was investigated by scientists from GSK.⁵⁶ From two PROTAC derivatives of ibrutinib/IAP ligand (covalent PROTAC 2) and a reversible BTK inhibitor/IAP ligand (PROTAC 3), the authors found that treatment of THP-1 cells with the covalent PROTAC 2 did not cause any BTK degradation despite confirmed target engagement, and inhibited BTK activity merely to the same extent as non-PROTAC covalent modification of recombinant BTK in vitro. In contrast, reversible PROTAC 3 caused near-complete BTK level reduction with a DC_{50} of 200 nM. Additional investigation with another covalent PROTAC (PROTAC 4) that recruits the E3 ligase CRBN produced a similar degradation profile, thus confirming this finding. Interestingly, covalent PROTAC 4 caused degradation of the Src family kinases CSK and LYN. This is expected since it binds reversibly to these proteins lacking the conserved cysteine present in the BTK kinase domain. Together, these results demonstrate the critical effect of catalysis on PROTAC-induced targeted protein degradation, as well as on an enhanced selectivity profile when converting an inhibitor to a degrader. Using information from high-resolution crystal structures of palbociclib, ribociclib, and abemaciclib with CDK6, researchers at the Dana-Farber Cancer Institute designed a series of PROTACs that degrade both cyclin-dependent kinases 4 and 6 (CDK4/6) or selectively reduce either CDK4 or CDK6 levels.⁵⁷ As previously observed, the selected inhibitor, linker length, and linker composition influenced the degradation activity and selectivity. Among these PROTACs, BSJ-02-162 (palbociclib-based) potently degraded CDK4, CDK6, IKZF1, and IKZF3. BSJ-02-162 exhibited an enhanced anti-proliferation effect in MCL cell lines in comparison to BSJ-

03-204 (also palbociclib-based), which only degrades CDK4/6 or the warhead ligands. Independently, Zhao and Burgess reported dual degradation of CDK4/6, resulting in reduced levels of phosphorylated retinoblastoma protein (Rb) and cell cycle arrest, with PROTAC recruiting CRBN.⁵⁸

Since its discovery, impressive progress has been made in advancing the PROTAC technology from an *in vitro* proof of concept to the first *in vivo* mice model validation. However, whether the preclinical efficacy of PROTAC drugs will translate into human therapy in the clinic remains to be determined. To assess the potential preclinical efficacy of this class of molecules, a recent study evaluated the ability of PROTACs to induce protein depletion in large animals such as non-human primates (Bama pigs and rhesus monkeys).^{59a} A series of PROTACs targeting CRBN and FKBP12 via pomalidomide and rapamycin were synthesized. Among those compounds, RC32 caused FKBP12 degradation with subnanomolar DC_{50} after 12 h in cells. This potent FKBP12 degradation was observed in different cell lines from different species. Further investigation revealed that RC32 treatment of mice twice a day (30 mg/kg, *ip*) caused complete knockdown of FKBP12 in different organs. The lack of FKBP12 degradation observed in the mice brain was attributed to the inability of RC32 to cross the blood-brain barrier. This finding is not surprising given the physicochemical properties of PROTAC molecules, which often possess a very high surface polar area. The ability of RC32 to induce FKBP12 degradation was further validated in the rhesus monkey model species that is closely related to humans. RC32 caused nearly complete degradation of FKBP12 in different rhesus monkey organs. Moreover, functional heart studies of the monkeys after RC32 administration (8 mg/kg, *ip*, twice a day) led to reduced ejection fraction (6.7% diminution at day 15) and fractional shortening (13.4% reduction at day 15) in accordance with the reduced systolic blood pressure found in RC32-treated monkeys. This effect was found to be reversible after withdrawal of the treatment. Taken in its entirety, this work demonstrated that PROTACs can indeed produce targeted protein degradation in species closely related to humans, thus strongly demonstrating their clinical potential.^{59a} The U.S. Food and Drug Administration (FDA) has recently cleared Arvinas's investigational new drug application (IND) for their oral PROTAC degrader ARV-110 against metastatic castration-resistant prostate cancer (mCRPC).^{59b} Thus, this entire research field is eager to learn how PROTACs will behave in these first clinical trials (Table 1).^{60–104}

1.3. Linkers and Exit Vectors

PROTACs have two recognition elements (heads), one of them specific to the protein of interest and the other to an E3 ligase, and these two heads are separated by a linker. The nature and size of the linker plays an important role in determining the right distance and appropriate physicochemical properties of the entire molecule.¹⁰⁵ The linkers should be long enough to prevent steric clashes between the two proteins. However, if they get too long, the systems would suffer from solubility and

physicochemical issues as well as linker folding. The importance of the length and nature of the linker was previously highlighted by the selective degradation of BRD4 over BRD2/BRD3—all members of the BET family of proteins—with a warhead that has nearly equivalent binding to several other BRD subtypes such as BRD2/3/4.²⁰ Independently, Nowak et al. reported a similar finding, namely that ternary complex conformations are governed by linker length and composition, therefore affecting the degradation selectivity of target proteins.¹⁰⁶ These observations, were further validated by Crews and co-workers who targeted for degradation with a PROTAC a family member of the human epidermal growth factor receptor protein.⁸² Using the ligand lapatinib and recruiting the same E3 ligase VHL, but using two different linkers, PROTAC1, with a shorter linker length, efficiently degraded both EGFR and HER2, while PROTAC 5, with a longer linker, selectively degraded EGFR over HER2.⁸² Thus, varying PROTAC linkers can offer an extra layer of selectivity.

Very recently, Wang's research group reported that the linker could be manipulated to increase solubility and modulate the physicochemical properties of the final PROTAC compound, leading to more potent degraders.^{66,83} In a recent study, the position of the exit vector was also found to play a critical role in the degradation profile. Using the same BTK-binding ligand, same linker length, and recruiting the same E3 ligase but with different exit vectors, PROTAC MT-797, with attachment points at position 4 of the CRBN ligand pomalidomide, was not able to induce any BTK degradation, while MT-802 was found to be highly potent with D_{max} of 99% at 250 nM along with an impressive DC_{50} of 9.1 nM.⁷⁷ Crews and collaborators reported on their progress in compound design and target selection, leading to the preparation of fewer yet more effective molecules, across different classes of proteins.⁹² For example, using the same VHL E3-ligase ligand and same p38 ligand (foretinib), but varying the exit vector and/or the linker length, they were able to selectively degrade isoenzymes p38 α or p38 δ . SJF-8240, having a 12-atom linker, was more selective for p38 α (DC_{50} of 7.16 ± 1.03 nM and D_{max} of 97.4%), whereas it had only a D_{max} of 18% and DC_{50} of 299 nM for p38 δ . Moreover, it was not able to degrade isoforms β and γ of p38. In contrast, SJF δ , with a shorter linker (10 atoms) and a different VHL ligand, successfully degraded p38 δ with a D_{max} of $99.41 \pm 3.31\%$ and DC_{50} of 46.17 ± 9.85 nM, but could not degrade the α , β , or γ isoforms of p38. This impressive enzyme isoform degradation selectivity is driven by differential target presentation, leading to one productive ternary complex that is dependent on the exit vector selected and the linker length. Collectively, these studies have demonstrated that linkers and exit vectors can affect the physicochemical properties, selectivity, and even degradation profiles of PROTACs.

2. PROTAC Library Design

After more than 15 years of research, PROTAC design remains a highly complex and mostly empirical task. At present, discovery is centered around known ligands that are utilized as the

handle to recruit the target protein. These ligands are usually well-characterized inhibitors with known structure-activity relationships and/or crystal structures, which helps to identify suitable attachment points for linkers and provides rational starting points for exit vectors. It is important to note that the chosen ligand can severely impact the degradation potential of the PROTAC itself. One study showed that bosutinib- and dasatinib-based PROTACs²² exhibit different ABL degradation

profiles despite possessing similar binding modes and exit vectors. In the case where one has several chemical series to choose the target ligand from, one should be aware that these subtle changes influence the degradation profile. Usually, only few ligands are of interest either due to their physicochemical properties or ADME profile. If possible, one should choose a ligand that has no liabilities here since they could make the optimization of the corresponding PROTAC very challenging.

Table 1. Cellular Protein Degraders

| Protein Target | Target Class | Compound | Reference |
|-----------------------------|---------------------------------|---|----------------------------|
| ABL, BCR-ABL | Tyr Kinase | DAS-6-2-2-6-CRBN | 22 |
| Akt | Ser/Thr kinase | Tri_a-PROTAC | 60 |
| ALK | Tyr Kinase | TL13-112, MS-4077, MS-4078, TD-004 | 61–63 |
| α -synuclein | brain protein | TAT- β synCTM | 64 |
| AR | nuclear receptor | I κ B α -DHT PROTAC, PROTAC 5, PROTAC A, SARM nutlin, ARCC-4, ARD-69, Compound 42a, SARD279, SNIPER 11 | 24, 25, 28, 30, 65–69 |
| ARH | transcription factor | Apigenin PROTAC | 70 |
| BCL6 | transcription factor | Compound 15 | 50 |
| BET (BRD2, BRD3, BRD4) | bromodomain | ARV-825, MZ1, dBET1, ARV-771, BETd-260/ZBC260, QCA570 | 18, 20, 21, 23, 71–74 |
| BRD7, BRD9 | bromodomain | VZ185 | 75 |
| BRD9 | bromodomain | dBRD9 | 76 |
| BTK | Tyr kinase | Compound 10, CJH-005-067, DD-04-015, MT-802 | 41, 44, 77 |
| CAPER α | splicing factor | E7820, Indisulam, CQS | 78 |
| CDK6 | cyclin-dependent kinase | BSJ-03-123 | 79 |
| CDK9 | cyclin-dependent kinase | Compound 3, Compound 11c | 80, 81 |
| cMet | RTK | Compound 7 | 82 |
| CRABP | nuclear receptor | Compound 4b | 31 |
| DAPK1 | Ser/Thr kinase | TAT-GluN2BCTM | 64 |
| EGFR | RTK | Compound 1 (also 3-5) | 82 |
| ER | nuclear receptor | I κ B α Phosphopeptide-estradiol PROTAC, E2-SMPI, PROTAC B, SNIPER 9, ERD-308, TD-PROTAC, Compounds 5-7 | 24, 26, 28, 69, 83, 84, 85 |
| ERK1/2 | Ser/Thr kinase | ERK-ClipTac | 86 |
| ERR α | nuclear receptor | PROTAC_ERR α | 19 |
| Fak | Tyr kinase | PROTAC-3 | 51 |
| FKBP12 _{F36V} | prolyl isomerase | PROTAC 4, dTag-13 | 25, 87 |
| FLT-3 | RTK | TL13-117, TL13-149, FLT-3 PROTAC | 44, 46 |
| FRS2 α | growth receptor | phosphoPROTAC ^{TrkA} PP _{FRS2α} | 29 |
| HaloTag [®] | fusion tag | HaloPROTAC 3 | 88 |
| HDAC6 | deacetylase | dHDAC6 | 89 |
| Her2 | RTK | Compound 1 | 82 |
| Huntington | disease protein | 60Q-HSC70bm | 90 |
| MDM2 | E3 ligase | MD-224 | 91 |
| MetAP2 | aminopeptidase | I κ B α -OVA PROTAC, Fu-SMPI | 4, 26 |
| p38 α , p38 δ | Ser/Thr kinase | SJF α , SJF δ | 92 |
| PARP1 | transferase | Compound 3 | 53 |
| PCAF/GCN5 | bromodomain | GSK983 | 93 |
| PI3K | kinase | phosphoPROTAC ^{ErbB2} PP _{PI3K} , Compound D | 29, 94 |
| Pirin | cupin family | CCT367766 | 49 |
| Plk1 | Ser/Thr kinase | Poloxin-2HT | 95 |
| PSD-95 | scaffolding protein | TAT-GluN2B9cCTM | 64 |
| RAR | nuclear receptor | SNIPER 13 | 69 |
| RBM39 | splicing factor | Indisulam, Tasisulam, CQS | 96 |
| RIP2K | Ser/Thr kinase | PROTAC_RIP2k | 19 |
| Sirt2 | lysine deacetylase | Compound 12 | 97 |
| Smad3 | DNA binding protein | PROTAC | 98 |
| TACC3 | spindle regulatory protein | SNIPER(TACC3) | 99 |
| Tau | microtubuli stabilizing protein | Peptide 1, TH006 | 100, 101 |
| TBK1 | Ser/Thr kinase | Compound 3i | 102 |
| VHL | E3 ligase | CM11, Homo-PROTAC | 103 |
| X-protein | viral protein | | 104 |

Moreover, crystal structures of targets and E3 ligases that have been used to model the ternary complex provide a retrospective justification to degradation and target selectivity.² The first effort to use computation to predict the ternary complex³ and the evolution of this effort will increasingly guide PROTAC design in the future. Until then, researchers must synthesize a permuted library consisting of different E3 ligase binders; linkers with diverse lengths, compositions, and exit vectors; and appropriate protein binders. Coverage of all this synthetic diversity can easily add up to 100+ PROTACs being synthesized for an initial degradation screen to find out if a target is amenable to the approach or not.

Since resources at the proof-of-concept stage or for early projects are usually limited in industry and academia, multistep syntheses and laborious testing of large compound sets to fully explore PROTAC options can set a high barrier to overcome. To help facilitate such efforts, PROTAC building blocks and Partial Degraders have recently become commercially available. They consist of E3 ligase binders that are connected to linkers of various lengths and with different reactive groups that allow for flexible conjugation chemistry (**Figure 4**). The use of such templates reduces degrader synthesis to a one-step reaction between the building block and the target ligand precursor.

Currently, only binders for CRBN and VHL are available as they are the best studied. For CRBN, pomalidomide-derived building blocks are offered because of their synthetic accessibility. For VHL, modification of the amide group of the

VHL ligand leads to accessible derivatives. Linkers are usually based on PEG or alkyl chains, and contain up to 6 ethylene glycol units. Longer linkers have not shown any improvement so far,^{4b} and researchers can limit their efforts to utilizing 5–25 atoms. In contrast to PEG chains, which increase the solubility and decrease the lipophilicity of the PROTAC, alkyl chains cause the PROTAC to become more insoluble and lipophilic as the size of the alkyl chain increases. This provides researchers with a first handle to tune PROTAC properties. After examining the published *in vivo* active compounds, one often finds rigidified linkers possessing piperazine, phenyl, or spirocyclic motifs. Although these linkers have better ADME properties, we do not recommend using them at the degrader discovery stage. Floppy PEG or alkyl chains can adopt multiple conformations, increasing the likelihood of finding a degrader. Once a degrader with an optimal linker length is found, optimization of the linker composition and rigidity can be started.

Moreover, the portfolio of available reactive groups is expanding steadily. Traditionally, first compound design started with amide-bond formation, since carboxylic acid and amide building blocks are readily available. Additionally, click chemistry has proven valuable in PROTAC research,^{5–8} and, thus, azide and alkyne building blocks are emerging as good options. Additionally, alkyne derivatives can be employed in Sonogashira couplings with aryl halide containing precursors. This diversity in conjugation reactions increases the applicability of the technology and provides a first tool to tune the angle of

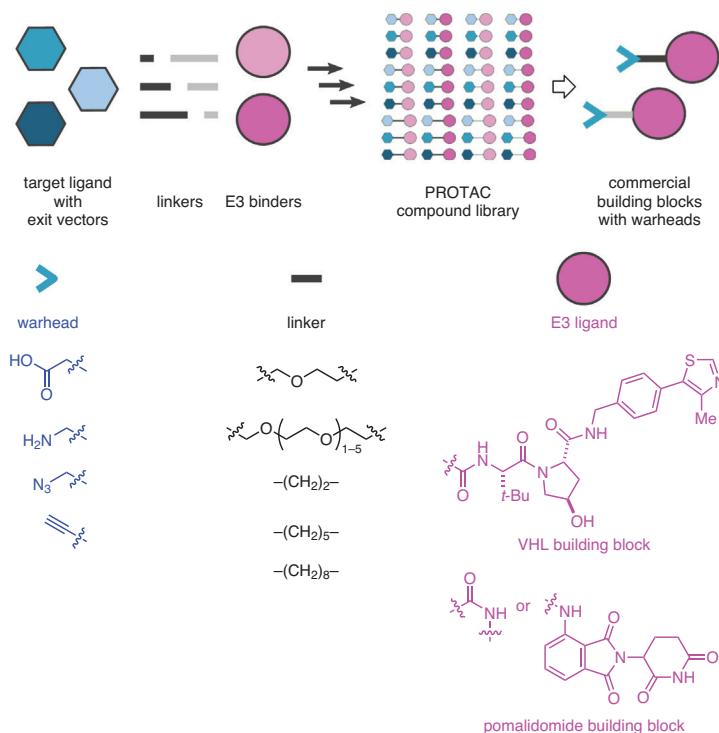


Figure 4. PROTAC Discovery Remains Empirical, and Designed Libraries Rely on Permutations of Target Ligands, Linkers, and E3 Binders.

the PROTAC's exit vector on the target protein side. From a pragmatic point of view, one should start with the conjugation chemistry that is most convenient and gives the fastest results.

Having all these available options, researchers can easily design their first set of PROTAC molecules from their target ligands of choice. The set could consist of a hundred members for an in-depth analysis of the degrader potential or of only a dozen members for a proof-of-concept study. At a minimum, the set should consist of at least five members of different lengths per E3 ligase and target ligand to cover the main aspects of PROTAC design. Such a set would yield well-balanced molecules with sufficient solubility, stability, and permeability to allow initial testing in degradation assays. As demonstrated by recent examples of testing in vivo, compound optimization is also possible, since the "rule-of-5" applies similarly to PROTAC set design⁴⁹ and provides chemists with a basis for improving compounds in the set. However, adherence to the "rule-of-5" holistically by all PROTAC degraders in development may vary and should be kept in mind. In addition, further optimization of the set could include using optimized E3 ligands, variation of their exit vectors, linker composition and rigidity with focus on improved ADME profile, as well as target ligand exit vectors, and should be accompanied by straightforward compound profiling.

3. Profiling of PROTAC Compounds

Having the PROTAC library in hand, member compounds can be profiled for target binding and degradation. In addition to state-of-the-art optimization of physicochemical and ADME parameters, in-depth profiling of the degradation process, kinetics, and selectivity can be used to optimize the molecules to create an efficacious in vivo degrader. An example of a screening cascade is depicted in Figure 5.

3.1. Binding Confirmation

When the exit vector of the ligand is unknown, the unmodified ligand could be used as a relative baseline for binding. To screen the PROTAC library for target binding, various binding assays, such as the Surface Plasmon Resonance (SPR) assay, may be utilized. For enzyme targets such as kinases, an enzymatic assay can also serve this purpose if an inhibitor is employed as the target handle. Comparing the K_D or IC_{50} of the PROTAC being tested to the unmodified ligand gives a measure of how well the linker position is accepted. If the K_D or IC_{50} is within 20-fold, that can be reasonable evidence that the exit vector on the PROTAC assayed is tolerated. It should be noted, however, that the binding affinity between the PROTAC and target often does not correlate to how effectively the PROTAC will degrade that target; for example, micromolar binding can still yield an active PROTAC.⁴²

3.2. Degradation Assay

The most important assay is a degrader assay performed to investigate the ability of a PROTAC compound to induce target degradation by quantifying the changes in intracellular protein levels. Important parameters determined include DC_{50} , the

concentration at which half of the protein is degraded; D_{max} , the maximal degradation reported as a percentage level; and t_{max} , the time frame at D_{max} (Figure 6, Part (a)). Additionally, a good degradation assay should take into consideration other factors such as cell lines used, concentrations applied, incubation times, control experiments, and method of detection.

3.2.1. Choosing a Cell Line

The cell line chosen should be easy to handle and specific to the phenotype or therapeutic application of the PROTAC target, e.g., cancer cell lines for cancer targets. Moreover, if unknown, the target and E3 expression levels should be sufficiently high or tested beforehand. Ideally, a cell line is chosen that permits further testing, such as proliferation or phenotypic assays, to be performed according to established protocols. However, one can also start with an easy-to-treat cell line such as HEK293, HeLa, or Jurkat and test only optimized compounds in more complex cells such as 3D cultures, co-cultures, or primary cells.

3.2.2. Effect of PROTAC Concentration on Assay

PROTACs should be tested in a concentration range. If concentrations are too low, there may not be enough PROTAC to bring together the ternary complex. If concentrations are too high, elevated levels of PROTAC could preclude complex formation due to saturation of the individual target and E3 ligase binding sites (hook effect; see Figure 6, Part (b)).¹⁹ This is drastically different from traditional assay development that usually starts with the highest concentration possible. With PROTACs, the reported DC_{50} values range from sub-nM to 100 μ M. For hit discovery, three PROTAC concentrations are recommended: 0.1, 1, and 10 μ M. At higher concentrations, small-molecule PROTACs can suffer from solubility issues.

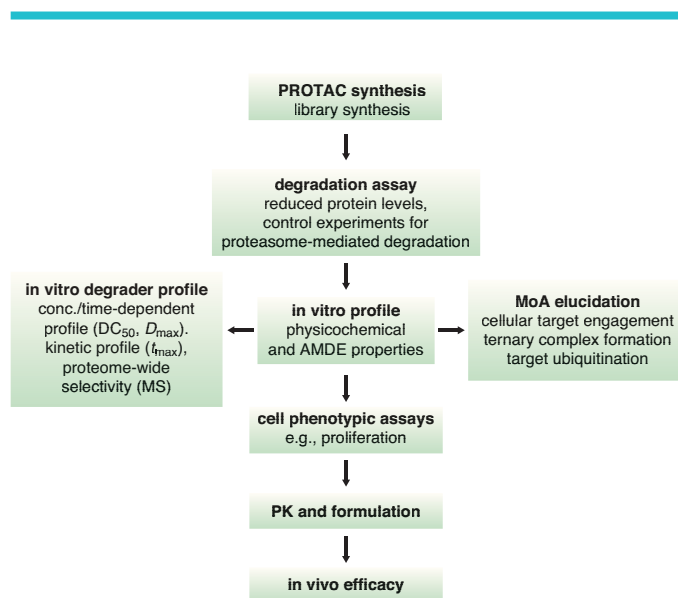


Figure 5. Example of a PROTAC Degradation Screening Cascade.

3.2.3. Assay Time Points

Ideally, assay time points are guided by knowledge about target turnover and re-synthesis rate. It is recommended that different incubation times be investigated during hit discovery for targets with unknown turnover. If the wrong incubation period is chosen, the protein may have already been re-synthesized, and then the PROTAC compound may appear inactive.¹⁰⁷ Moreover, the testing of different incubation times gives preliminary insights into the degradation kinetics, which is helpful for PROTAC optimization.

3.2.4. Assay Controls

Several assay controls have been described in the literature. Frequently, proteasome inhibitors such as carfilzomib,⁴⁴ epoxomicin,⁷⁷ MG132,⁹⁸ and 17-AAG⁸² are employed. They prevent target protein degradation by the proteasome, and result in the reconstitution of untreated protein levels. In many cases, the respective E3 ligand⁷⁷ is added as a competitor in high concentrations. This suppresses the binding of the PROTAC to its E3 ligase, and thus degradation levels are reduced. Commonly, an inactive PROTAC with similar physicochemical properties is employed, but is unable to bind its E3 ligase. In the case of VHL, this is achieved by incorporating the inactive *S*-enantiomer⁶⁵ into the PROTAC. For CRBN, methylated⁹¹ or de-oxygenated⁶¹ thalidomide analogues are used. In the case of cullin RING ligases such as CRBN and VHL, the NEDD8

inhibitor MLN4924⁶² can also be utilized since neddylation is essential for the activation of cullin RING ligases (CRLs). If such controls do not reduce the degradation effect, the tested PROTAC is very likely inducing nonspecific degradation effects such as destabilization or autophagy.¹⁰⁸

Lastly, a few reports have shown that siRNA can also be used as a control. If siRNA is directed against the E3 ligase,⁸¹ degradation is abolished. Similarly, siRNA against the target¹⁰⁰ can be a suitable control for phenotypes with reduced protein levels.

3.2.5. Protein Detection Methods

Western blotting is the current method of choice in the PROTAC field to determine protein levels due to its ease in handling, the availability of established protocols, and its few requirements (i.e., no need for genetic manipulation and expensive instrumentation). The cells are incubated with a PROTAC compound prior to lysis, and the proteome is analyzed by SDS-PAGE and blotted to a membrane. A target-specific antibody and a suitable secondary antibody are chosen that allow for fluorescent or chemiluminescent readout of the target protein. A second, unaffected protein such as GADPH,⁸³ actin,⁵³ tubulin,⁶⁵ vinculin⁸⁷ or histone 3⁷⁹ is detected in parallel as a loading control, providing a quantitative readout of the overall protein level in the sample. In this way, degradation effects can be investigated in a concentration and time-

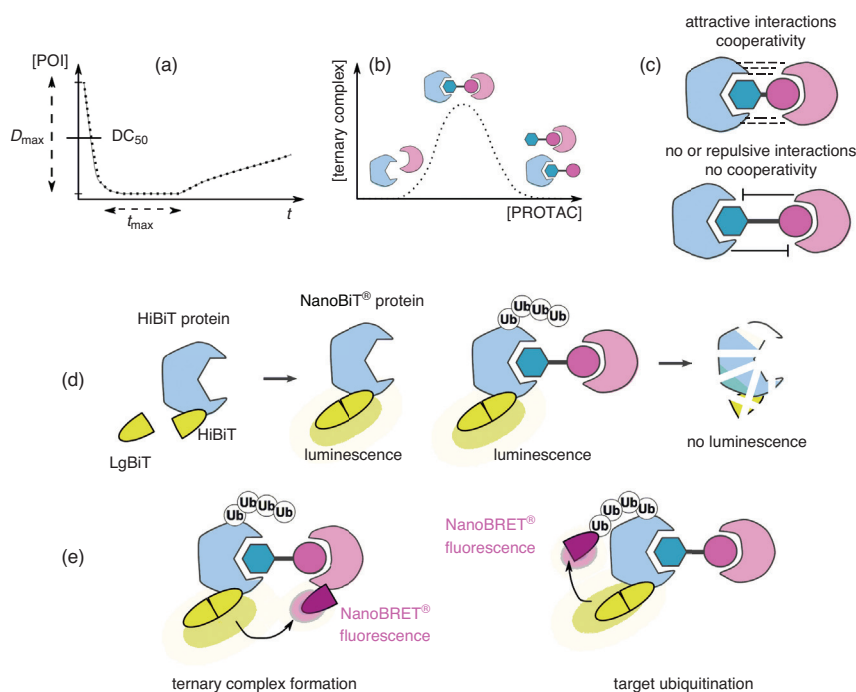


Figure 6. (a) Time-Course of Protein Levels during Induced Degradation. Parameters Measured Are DC_{50} , D_{max} , and t_{max} . (b) Ternary Complex Formation Dependence on PROTAC Concentration. High Concentrations Lead to Unproductive Dimers "Hook-Effect". (c) Cooperativity in Ternary Complexes. (d) NanoBiT® Technology to Quantify Protein Levels. (e) NanoBRET® Technology to Quantify Ternary Complex Formation and Target Ubiquitination.

dependent manner. Likewise, mass spectrometry^{42,44,109} has been applied to quantify cellular degradation effects. By combining dynamic-SILAC labeling with isobaric mass tagging, proteome-wide protein levels could be investigated, allowing the additional assessment of PROTAC selectivity and whole proteasome effects.

However, the preparation of cell lysates can be very laborious when performed in high-throughput, e.g., when screening a library of PROTAC compounds. To overcome this, several reports have been published that use fusion proteins to determine protein levels. In some reports, GFP-tagged target proteins are employed,^{20,25,64,88} and the relative fluorescence is correlated with protein levels, measurable by flow cytometry¹⁰⁰ or a multiwell-plate reader.³⁷ Thus, a decrease in fluorescence would indicate a decrease in protein levels. Similarly, a luciferase fusion protein^{75,79,96,107} can be employed to detect protein levels by chemiluminescence. Notably, one study¹⁰⁷ compared the PROTAC-induced degradation of transiently expressed fusion proteins with stably expressed fusion proteins and found that parameters measured from ectopic expressions are skewed due to overexpression and missing epigenetic and transcriptional control mechanisms. Consequently, only stably expressed fusion proteins should be utilized for the quantitative interpretation of protein levels and degradation parameters.

3.3. Kinetic Profiling and MoA Studies of Degraders

Targeting a protein for degradation is a highly complex process where the PROTAC molecule can fail in any of several steps. After the degrader molecule enters the cell, it binds to its target and E3 ligase to form a ternary complex that enables the transfer of multiple ubiquitins to the target, thus sending it for lysis by the proteasome. In the case of inactive degraders, or to further optimize PROTACs, it can be beneficial to evaluate the early steps in the degradation process. For instance, a PROTAC might be impermeable⁴⁹ or bind more strongly to a second, undesired⁴³ target. To find out if that is the case, a cellular target engagement assay could be helpful. Another pitfall could be that the PROTAC cannot induce the formation of a ternary complex in cells, or it does so in a geometry that disfavors ubiquitination or selectivity.⁴⁰ Here, assays demonstrating ternary complex formation or target ubiquitination could provide further insight.

One particular assay with a potential to greatly contribute to the PROTAC field was recently developed by Daniels and co-workers at Promega.¹⁰⁷ They combined endogenous tagging with NanoBiT® technology to enable the quantitative measurement of protein levels and to investigate the kinetics of target degradation in living cells (Figure 6, Part (d)). The same researchers used CRISPR/Cas9 genome editing^{110,111} to insert an 11 amino acid peptide, termed HiBiT, into the protein of interest. Similarly, researchers at Promega and the University of Utah introduced an 18 kDa protein, called LgBiT, that spontaneously assembles with pM affinity to form the functional NanoBiT® luciferase.^{112,113} Using bioluminescence imaging, they were able to monitor the degradation profile in

real-time with quantitation of degradation parameters such as DC_{50} , D_{max} , and t_{max} . Next, they established a NanoBRET®¹¹⁴ protocol with ectopically expressed HaloTag® fusion proteins of the E3 ligases⁸⁸ and ubiquitin as energy acceptors. When a PROTAC induces proximity between the NanoBiT®-tagged target protein and the HaloTag®-E3 ligase or HaloTag®-ubiquitin, energy transfer occurs and results in a fluorescent signal (Figure 6, Part (e)). Thus, intracellular ternary complex formation and target ubiquitination were investigated in a time-dependent manner.

A few crystal structures^{40,50,75,106} have been published that broaden our understanding of the structural features of ternary complexes. It was found that some protein-protein interactions can lead to a cooperative effect^{40,41,115} (Figure 6, Part (c)) that turns a PROTAC into an efficient or a particularly selective degrader. Moreover, initial attempts to rationalize PROTAC design and to identify these cooperative interactions by in silico prediction have been published, and will likely evolve with further understanding of the technology.^{45,106}

4. Conclusion

Targeted protein degradation is a rapidly growing research area that has evolved within the last decade from a purely academic research tool into a therapeutic modality that is of great interest in industry as well as academia. With the first PROTACs entering clinical trials in 2019, researchers will be keen to find out if PROTACs will keep their promise, and what some of the limitations on their use may be. The list of targets amenable to this approach has been steadily growing, and scientific efforts to expand the scope of suitable E3 ligands, clever assay development, future prediction tools, as well as commercially available building blocks and kits will further advance the technology and facilitate its application to tomorrow's medicines.

5. References

- (1) Coleman, K. G.; Crews, C. M. *Annu. Rev. Cancer Biol.* **2018**, *2*, 41.
- (2) Lai, A. C.; Crews, C. M. *Nat. Rev. Drug Discovery* **2017**, *16*, 101.
- (3) Toure, M.; Crews, C. M. *Angew. Chem., Int. Ed.* **2016**, *55*, 1966.
- (4) (a) Mayor-Ruiz, C.; Winter, G. E. *Drug Discovery Today: Technol.* **2019**, *31*, 81. (b) Sakamoto, K. M.; Kim, K. B.; Kumagai, A.; Mercurio, F.; Crews, C. M.; Deshaies, R. J. *Proc. Natl. Acad. Sci. U. S. A.* **2001**, *98*, 8554.
- (5) Hopkins, A. L.; Groom, C. R. *Nat. Rev. Drug Discovery* **2002**, *1*, 727.
- (6) Clamp, M.; Fry, B.; Kamal, M.; Xie, X.; Cuff, J.; Lin, M. F.; Kellis, M.; Lindblad-Toh, K.; Lander, E. S. *Proc. Natl. Acad. Sci. U. S. A.* **2007**, *104*, 19428.
- (7) Burnett, J. C.; Rossi, J. J. *Chem. Biol.* **2012**, *19*, 60.
- (8) Wishart, D. S.; Knox, C.; Guo, A. C.; Shrivastava, S.; Hassanali, M.; Stothard, P.; Chang, Z.; Woolsey, J. *Nucleic Acids Res.* **2006**, *34*, D668.
- (9) Rinaldi, C.; Wood, M. J. A. *Nat. Rev. Neurol.* **2018**, *14*, 9.
- (10) Zamecnik, P. C.; Stephenson, M. L. *Proc. Natl. Acad. Sci. U. S. A.* **1978**, *75*, 280.

- (11) Doudna, J. A.; Charpentier, E. *Science* **2014**, *346*, 1077.
- (12) Hsu, P. D.; Lander, E. S.; Zhang, F. *Cell* **2014**, *157*, 1262.
- (13) Sander, J. D.; Joung, J. K. *Nat. Biotechnol.* **2014**, *32*, 347.
- (14) De Smidt, P. C.; Le Doan, T.; de Falco, S.; van Berkel, T. J. C. *Nucleic Acids Res.* **2007**, *19*, 4695.
- (15) Jackson, A. L.; Bartz, S. R.; Schelter, J.; Kobayashi, S. V.; Burchard, J.; Mao, M.; Li, B.; Cavet, G.; Linsley, P. S. *Nat. Biotechnol.* **2003**, *21*, 635.
- (16) Iyer, V.; Boroviak, K.; Thomas, M.; Doe, B.; Riva, L.; Ryder, E.; Adams, D. J. *PLoS Genet.* **2018**, *14* (7), e1007503 (DOI: 10.1371/journal.pgen.1007503).
- (17) Fu, Y.; Foden, J. A.; Khayter, C.; Maeder, M. L.; Reyon, D.; Joung, J. K.; Sander, J. D. *Nat. Biotechnol.* **2013**, *31*, 822.
- (18) Lu, J.; Qian, Y.; Altieri, M.; Dong, H.; Wang, J.; Raina, K.; Hines, J.; Winkler, J. D.; Crew, A. P.; Coleman, K.; Crews, C. M. *Chem. Biol.* **2015**, *22*, 755.
- (19) Bondeson, D. P.; Mares, A.; Smith, I. E. D.; Ko, E.; Campos, S.; Miah, A. H.; Mulholland, K. E.; Routly, N.; Buckley, D. L.; Gustafson, J. L.; Zinn, N.; Grandi, P.; Shimamura, S.; Bergamini, G.; Faelth-Savitski, M.; Bantscheff, M.; Cox, C.; Gordon, D. A.; Willard, R. R.; Flanagan, J. J.; Casillas, L. N.; Votta, B. J.; den Besten, W.; Famm, K.; Kruidenier, L.; Carter, P. S.; Harling, J. D.; Churcher, I.; Crews, C. M. *Nat. Chem. Biol.* **2015**, *11*, 611.
- (20) Zengerle, M.; Chan, K.-H.; Ciulli, A. *ACS Chem. Biol.* **2015**, *10*, 1770.
- (21) Winter, G. E.; Buckley, D. L.; Paulk, J.; Roberts, J. M.; Souza, A.; Dhe-Paganon, S.; Bradner, J. E. *Science* **2015**, *348*, 1376.
- (22) Lai, A. C.; Toure, M.; Hellerschmied, D.; Salami, J.; Jaime-Figueroa, S.; Ko, E.; Hines, J.; Crews, C. M. *Angew. Chem., Int. Ed.* **2016**, *55*, 807.
- (23) Raina, K.; Lu, J.; Qian, Y.; Altieri, M.; Gordon, D.; Rossi, A. M. K.; Wang, J.; Chen, X.; Dong, H.; Siu, K.; Winkler, J. D.; Crew, A. P.; Crews, C. M.; Coleman, K. G. *Proc. Natl. Acad. Sci. U. S. A.* **2016**, *113*, 7124.
- (24) Sakamoto, K. M.; Kim, K. B.; Verma, R.; Ransick, A.; Stein, B.; Crews, C. M.; Deshaies, R. J. *Mol. Cell. Proteomics* **2003**, *2*, 1350.
- (25) Schneckloth, J. S., Jr.; Fonseca, F. N.; Koldobskiy, M.; Mandal, A.; Deshaies, R.; Sakamoto, K.; Crews, C. M. *J. Am. Chem. Soc.* **2004**, *126*, 3748.
- (26) Zhang, D.; Baek, S.-H.; Ho, A.; Kim, K. *Bioorg. Med. Chem. Lett.* **2004**, *14*, 645.
- (27) Lee, H.; Puppala, D.; Choi, E.-Y.; Swanson, H.; Kim, K.-B. *ChemBioChem* **2007**, *8*, 2058.
- (28) Rodriguez-Gonzalez, A.; Cyrus, K.; Salcius, M.; Kim, K.; Crews, C. M.; Deshaies, R. J.; Sakamoto, K. M. *Oncogene* **2008**, *27*, 7201.
- (29) Hines, J.; Gough, J. D.; Corson, T. W.; Crews, C. M. *Proc. Natl. Acad. Sci. U. S. A.* **2013**, *110*, 8942.
- (30) Schneckloth, A. R.; Pucheault, M.; Tae, H. S.; Crews, C. M. *Bioorg. Med. Chem. Lett.* **2008**, *18*, 5904.
- (31) Itoh, Y.; Ishikawa, M.; Naito, M.; Hashimoto, Y. *J. Am. Chem. Soc.* **2010**, *132*, 5820.
- (32) Buckley, D. L.; van Molle, I.; Gareiss, P. C.; Tae, H. S.; Michel, J.; Noblin, D. J.; Jorgensen, W. L.; Ciulli, A.; Crews, C. M. *J. Am. Chem. Soc.* **2012**, *134*, 4465.
- (33) Buckley, D. L.; Gustafson, J. L.; van Molle, I.; Roth, A. G.; Tae, H. S.; Gareiss, P. C.; Jorgensen, W. L.; Ciulli, A.; Crews, C. M. *Angew. Chem., Int. Ed.* **2012**, *51*, 11463.
- (34) Van Molle, I.; Thomann, A.; Buckley, D. L.; So, E. C.; Lang, S.; Crews, C. M.; Ciulli, A. *Chem. Biol.* **2012**, *19*, 1300.
- (35) Galdeano, C.; Gadd, M. S.; Soares, P.; Scaffidi, S.; van Molle, I.; Birced, I.; Hewitt, S.; Dias, D. M.; Ciulli, A. *J. Med. Chem.* **2014**, *57*, 8657.
- (36) Chamberlain, P. P.; Lopez-Girona, A.; Miller, K.; Carmel, G.; Pagarigan, B.; Chie-Leon, B.; Rychak, E.; Corral, L. G.; Ren, Y. J.; Wang, M.; Riley, M.; Delker, S. L.; Ito, T.; Ando, H.; Mori, T.; Hirano, Y.; Handa, H.; Hakoshima, T.; Daniel, T. O.; Cathers, B. E. *Nat. Struct. Mol. Biol.* **2014**, *21*, 803.
- (37) Fischer, E. S.; Böhm, K.; Lydeard, J. R.; Yang, H.; Stadler, M. B.; Cavadini, S.; Nagel, J.; Serluca, F.; Acker, V.; Lingaraju, G. M.; Tichkule, R. B.; Schebesta, M.; Forrester, W. C.; Schirle, M.; Hassiepen, U.; Ottl, J.; Hild, M.; Beckwith, R. E. J.; Harper, J. W.; Jenkins, J. L.; Thomä, N. H. *Nature* **2014**, *512*, 49.
- (38) Krönke, J.; Udeshi, N. D.; Narla, A.; Grauman, P.; Hurst, S. N.; McConkey, M.; Svinkina, T.; Heckl, D.; Comer, E.; Li, X.; Ciarlo, C.; Hartman, E.; Munshi, N.; Schenone, M.; Schreiber, S. L.; Carr, S. A.; Ebert, B. L. *Science* **2014**, *343*, 301.
- (39) Lu, G.; Middleton, R. E.; Sun, H.; Naniong, M.; Ott, C. J.; Mitsiades, C. S.; Wong, K.-K.; Bradner, J. E.; Kaelin, W. G., Jr. *Science* **2014**, *343*, 305.
- (40) Gadd, M. S.; Testa, A.; Lucas, X.; Chan, K.-H.; Chen, W.; Lamont, D. J.; Zengerle, M.; Ciulli, A. *Nat. Chem. Biol.* **2017**, *13*, 514.
- (41) Zorba, A.; Nguyen, C.; Xu, Y.; Starr, J.; Borzilleri, K.; Smith, J.; Zhu, H.; Farley, K. A.; Ding, W.; Schiemer, J.; Feng, X.; Chang, J. S.; Uccello, D. P.; Young, J. A.; Garcia-Irrizary, C. N.; Czabaniuk, L.; Schuff, B.; Oliver, R.; Montgomery, J.; Hayward, M. M.; Coe, J.; Chen, J.; Niosi, M.; Luthra, S.; Shah, J. C.; El-Kattan, A.; Qiu, X.; West, G. M.; Noe, M. C.; Shanmugasundaram, V.; Gilbert, A. M.; Brown, M. F.; Calabrese, M. F. *Proc. Natl. Acad. Sci. U. S. A.* **2018**, *115*, E7285.
- (42) Bondeson, D. P.; Smith, B. E.; Burslem, G. M.; Buhimschi, A. D.; Hines, J.; Jaime-Figueroa, S.; Wang, J.; Hamman, B. D.; Ishchenko, A.; Crews, C. M. *Cell Chem. Biol.* **2018**, *25*, 78.
- (43) Ishoe, M.; Chorn, S.; Singh, N.; Jaeger, M. G.; Brand, M.; Paulk, J.; Bauer, S.; Erb, M. A.; Parapatics, K.; Müller, A. C.; Bennett, K. L.; Ecker, G. F.; Bradner, J. E.; Winter, G. E. *ACS Chem. Biol.* **2018**, *13*, 553.
- (44) Huang, H.-T.; Dobrovolsky, D.; Paulk, J.; Yang, G.; Weisberg, E. L.; Doctor, Z. M.; Buckley, D. L.; Cho, J.-H.; Ko, E.; Jang, J.; Shi, K.; Choi, H. G.; Griffin, J. D.; Li, Y.; Treon, S. P.; Fischer, E. S.; Bradner, J. E.; Tan, L.; Gray, N. S. *Cell Chem. Biol.* **2018**, *25*, 88.
- (45) Drummond, M. L.; Williams, C. I. *J. Chem. Inf. Model.* **2019**, *59*, DOI 10.1021/acs.jcim.8b00872.
- (46) Burslem, G. M.; Song, J.; Chen, X.; Hines, J.; Crews, C. M. *J. Am. Chem. Soc.* **2018**, *140*, 16428.
- (47) Gu, S.; Cui, D.; Chen, X.; Xiong, X.; Zhao, Y. *BioEssays* **2018**, *40*, DOI 10.1002/bies.201700247.
- (48) Hines, J.; Lartigue, S.; Dong, H.; Qian, Y.; Crews, C. M. *Cancer*

- Res. **2018**, 79, 251.
- (49) Chessum, N. E. A.; Sharp, S. Y.; Caldwell, J. J.; Pasqua, A. E.; Wilding, B.; Colombano, G.; Collins, I.; Ozer, B.; Richards, M.; Rowlands, M.; Stubbs, M.; Burke, R.; McAndrew, P. C.; Clarke, P. A.; Workman, P.; Cheeseman, M. D.; Jones, K. J. *Med. Chem.* **2018**, 61, 918.
- (50) McCoull, W.; Cheung, T.; Anderson, E.; Barton, P.; Burgess, J.; Byth, K.; Cao, Q.; Castaldi, M. P.; Chen, H.; Chiarpardin, E.; Carbajo, R. J.; Code, E.; Cowan, S.; Davey, P. R.; Ferguson, A. D.; Fillery, S.; Fuller, N. O.; Gao, N.; Hargreaves, D.; Howard, M. R.; Hu, J.; Kawatkar, A.; Kemmitt, P. D.; Leo, E.; Molina, D. M.; O'Connell, N.; Petteruti, P.; Rasmusson, T.; Raubo, P.; Rawlins, P. B.; Ricchiuto, P.; Robb, G. R.; Schenone, M.; Waring, M. J.; Zinda, M.; Fawell, S.; Wilson, D. M. *ACS Chem. Biol.* **2018**, 13, 3131.
- (51) Cromm, P. M.; Samarasinghe, K. T. G.; Hines, J.; Crews, C. M. *J. Am. Chem. Soc.* **2018**, 140, 17019.
- (52) Kaur, T.; Menon, A.; Garner, A. L. *Eur. J. Med. Chem.* **2019**, 166, 339.
- (53) Zhao, Q.; Lan, T.; Su, S.; Rao, Y. *Chem. Commun.* **2019**, 55, 369.
- (54) Popow, J.; Arnhof, H.; Bader, G.; Berger, H.; Ciulli, A.; Covini, D.; Dank, C.; Gmaschitz, T.; Greb, P.; Karolyi-Oezguer, J.; Koegl, M.; McConnell, D. B.; Pearson, M.; Rieger, M.; Rinnenthal, J.; Roessler, V.; Schrenk, A.; Spina, M.; Steurer, S.; Trainor, N.; Traxler, E.; Wieshofer, C.; Zoephel, A.; Ettmayer, P. *J. Med. Chem.* **2019**, 62, 2508.
- (55) Papatzimas, J. W.; Gorobets, E.; Maity, R.; Muniyat, M. I.; MacCallum, J. L.; Neri, P.; Bahlis, N. J.; Derksen, D. J. *ChemRxiv* **2019**, 1, 1 (DOI: 10.26434/chemrxiv.7722359.v1).
- (56) Tinworth, C. P.; Lithgow, H.; Dittus, L.; Bassi, Z. I.; Hughes, S. E.; Muelbaier, M.; Dai, H.; Smith, I. E. D.; Kerr, W. J.; Burley, G. A.; Bantscheff, M.; Harling, J. D. *ACS Chem. Biol.* **2019**, 14, 342.
- (57) Jiang, B.; Wang, E. S.; Donovan, K. A.; Liang, Y.; Fischer, E. S.; Zhang, T.; Gray, N. S. *Angew. Chem., Int. Ed.* **2019**, 58, DOI 10.1002/anie.201901336.
- (58) Zhao, B.; Burgess, K. *Chem. Commun.* **2019**, 55, 2704.
- (59) (a) Sun, X.; Wang, J.; Yao, X.; Zheng, W.; Mao, Y.; Lan, T.; Wang, L.; Sun, Y.; Zhang, X.; Zhao, Q.; Zhao, J.; Xiao, R.-P.; Zhang, X.; Ji, G.; Rao, Y. *Cell Discovery* **2019**, 5, 1. (b) *Globe Newswire* [Online], Jan 4, 2019. <https://www.globenewswire.com/news-release/2019/01/04/1680835/0/en/Arvinas-Receives-Authorization-to-Proceed-for-its-IND-Application-for-PROTAC-Therapy-to-Treat-Patients-with-Metastatic-Castration-Resistant-Prostate-Cancer.html>.
- (60) Henning, R. K.; Varghese, J. O.; Das, S.; Nag, A.; Tang, G.; Tang, K.; Sutherland, A. M.; Heath, J. R. *J. Pept. Sci.* **2016**, 22, 196.
- (61) Powell, C. E.; Gao, Y.; Tan, L.; Donovan, K. A.; Nowak, R. P.; Loehr, A.; Bahcall, M.; Fischer, E. S.; Jänne, P. A.; George, R. E.; Gray, N. S. *J. Med. Chem.* **2018**, 61, 4249.
- (62) Zhang, C.; Han, X.-R.; Yang, X.; Jiang, B.; Liu, J.; Xiong, Y.; Jin, J. *Eur. J. Med. Chem.* **2018**, 151, 304.
- (63) Kang, C. H.; Lee, D. H.; Lee, C. O.; Du Ha, J.; Park, C. H.; Hwang, J. Y. *Biochem. Biophys. Res. Commun.* **2018**, 505, 542.
- (64) Fan, X.; Jin, W. Y.; Lu, J.; Wang, J.; Wang, Y. T. *Nat. Neurosci.* **2014**, 17, 471.
- (65) Salami, J.; Alabi, S.; Willard, R. R.; Vitale, N. J.; Wang, J.; Dong, H.; Jin, M.; McDonnell, D. P.; Crew, A. P.; Neklesa, T. K.; Crews, C. M. *Commun. Biol.* **2018**, 1, 100.
- (66) Han, X.; Wang, C.; Qin, C.; Xiang, W.; Fernandez-Salas, E.; Yang, C.-Y.; Wang, M.; Zhao, L.; Xu, T.; Chinnaswamy, K.; Delproposto, J.; Stuckey, J.; Wang, S. *J. Med. Chem.* **2019**, 62, 941.
- (67) Shibata, N.; Nagai, K.; Morita, Y.; Ujikawa, O.; Ohoka, N.; Hattori, T.; Koyama, R.; Sano, O.; Imaeda, Y.; Nara, H.; Cho, N.; Naito, M. *J. Med. Chem.* **2018**, 61, 543.
- (68) Gustafson, J. L.; Neklesa, T. K.; Cox, C. S.; Roth, A. G.; Buckley, D. L.; Tae, H. S.; Sundberg, T. B.; Stagg, D. B.; Hines, J.; McDonnell, D. P.; Norris, J. D.; Crews, C. M. *Angew. Chem., Int. Ed.* **2015**, 54, 9659.
- (69) Itoh, Y.; Kitaguchi, R.; Ishikawa, M.; Naito, M.; Hashimoto, Y. *Bioorg. Med. Chem.* **2011**, 19, 6768.
- (70) Puppala, D.; Lee, H.; Kim, K. B.; Swanson, H. I. *Mol. Pharmacol.* **2008**, 73, 1064.
- (71) Zhou, B.; Hu, J.; Xu, F.; Chen, Z.; Bai, L.; Fernandez-Salas, E.; Lin, M.; Liu, L.; Yang, C.-Y.; Zhao, Y.; McEachern, D.; Przybranowski, S.; Wen, B.; Sun, D.; Wang, S. *J. Med. Chem.* **2018**, 61, 462.
- (72) Qin, C.; Hu, Y.; Zhou, B.; Fernandez-Salas, E.; Yang, C.-Y.; Liu, L.; McEachern, D.; Przybranowski, S.; Wang, M.; Stuckey, J.; Meagher, J.; Bai, L.; Chen, Z.; Lin, M.; Yang, J.; Ziazadeh, D. N.; Xu, F.; Hu, J.; Xiang, W.; Huang, L.; Li, S.; Wen, B.; Sun, D.; Wang, S. *J. Med. Chem.* **2018**, 61, 6685.
- (73) Sun, B.; Fiskus, W.; Qian, Y.; Rajapakshe, K.; Raina, K.; Coleman, K. G.; Crew, A. P.; Shen, A.; Saenz, D. T.; Mill, C. P.; Nowak, A. J.; Jain, N.; Zhang, L.; Wang, M.; Khoury, J. D.; Coarfa, C.; Crews, C. M.; Bhalla, K. N. *Leukemia* **2018**, 32, 343.
- (74) An, S.; Fu, L. *EBioMedicine* **2018**, 36, 553.
- (75) Zoppi, V.; Hughes, S. J.; Maniaci, C.; Testa, A.; Gmaschitz, T.; Wieshofer, C.; Koegl, M.; Riching, K. M.; Daniels, D. L.; Spallarossa, A.; Ciulli, A. *J. Med. Chem.* **2019**, 62, 699.
- (76) Remillard, D.; Buckley, D. L.; Pault, J.; Brien, G. L.; Sonnett, M.; Seo, H.-S.; Dastjerdi, S.; Wühr, M.; Dhe-Paganon, S.; Armstrong, S. A.; Bradner, J. E. *Angew. Chem., Int. Ed.* **2017**, 56, 5738.
- (77) Buhimschi, A. D.; Armstrong, H. A.; Toure, M.; Jaime-Figueroa, S.; Chen, T. L.; Lehman, A. M.; Woyach, J. A.; Johnson, A. J.; Byrd, J. C.; Crews, C. M. *Biochemistry* **2018**, 57, 3564.
- (78) Uehara, T.; Minoshima, Y.; Sagane, K.; Sugi, N. H.; Mitsuhashi, K. O.; Yamamoto, N.; Kamiyama, H.; Takahashi, K.; Kotake, Y.; Uesugi, M.; Yokoi, A.; Inoue, A.; Yoshida, T.; Mabuchi, M.; Tanaka, A.; Owa, T. *Nat. Chem. Biol.* **2017**, 13, 675.
- (79) Brand, M.; Jiang, B.; Bauer, S.; Donovan, K. A.; Liang, Y.; Wang, E. S.; Nowak, R. P.; Yuan, J. C.; Zhang, T.; Kwiatkowski, N.; Müller, A. C.; Fischer, E. S.; Gray, N. S.; Winter, G. E. *Cell Chem. Biol.* **2019**, 26, 300.
- (80) Robb, C. M.; Contreras, J. I.; Kour, S.; Taylor, M. A.; Abid, M.; Sonawane, Y. A.; Zahid, M.; Murry, D. J.; Natarajan, A.; Rana, S. *Chem. Commun.* **2017**, 53, 7577.

- (81) Bian, J.; Ren, J.; Li, Y.; Wang, J.; Xu, X.; Feng, Y.; Tang, H.; Wang, Y.; Li, Z. *Bioorg. Chem.* **2018**, *81*, 373.
- (82) Burslem, G. M.; Smith, B. E.; Lai, A. C.; Jaime-Figueroa, S.; McQuaid, D. C.; Bondeson, D. P.; Toure, M.; Dong, H.; Qian, Y.; Wang, J.; Crew, A. P.; Hines, J.; Crews, C. M. *Cell Chem. Biol.* **2018**, *25*, 67.
- (83) Hu, J.; Hu, B.; Wang, M.; Xu, F.; Miao, B.; Yang, C.-Y.; Wang, M.; Liu, Z.; Hayes, D. F.; Chinnaswamy, K.; Delproposto, J.; Stuckey, J.; Wang, S. *J. Med. Chem.* **2019**, *62*, 1420.
- (84) Jiang, Y.; Deng, Q.; Zhao, H.; Xie, M.; Chen, L.; Yin, F.; Qin, X.; Zheng, W.; Zhao, Y.; Li, Z. *ACS Chem. Biol.* **2018**, *13*, 628.
- (85) Demizu, Y.; Okuhira, K.; Motoi, H.; Ohno, A.; Shoda, T.; Fukuhara, K.; Okuda, H.; Naito, M.; Kurihara, M. *Bioorg. Med. Chem. Lett.* **2012**, *22*, 1793.
- (86) Lebraud, H.; Wright, D. J.; Johnson, C. N.; Heightman, T. D. *ACS Cent. Sci.* **2016**, *2*, 927.
- (87) Nabet, B.; Roberts, J. M.; Buckley, D. L.; Paulk, J.; Dastjerdi, S.; Yang, A.; Leggett, A. L.; Erb, M. A.; Lawlor, M. A.; Souza, A.; Scott, T. G.; Vittori, S.; Perry, J. A.; Qi, J.; Winter, G. E.; Wong, K.-K.; Gray, N. S.; Bradner, J. E. *Nat. Chem. Biol.* **2018**, *14*, 431.
- (88) Buckley, D. L.; Raina, K.; Darricarrere, N.; Hines, J.; Gustafson, J. L.; Smith, I. E.; Miah, A. H.; Harling, J. D.; Crews, C. M. *ACS Chem. Biol.* **2015**, *10*, 1831.
- (89) Yang, K.; Song, Y.; Xie, H.; Wu, H.; Wu, Y.-T.; Leisten, E. D.; Tang, W. *Bioorg. Med. Chem. Lett.* **2018**, *28*, 2493.
- (90) Bauer, P. O.; Goswami, A.; Wong, H. K.; Okuno, M.; Kurosawa, M.; Yamada, M.; Miyazaki, H.; Matsumoto, G.; Kino, Y.; Nagai, Y.; Nukina, N. *Nat. Biotechnol.* **2010**, *28*, 256.
- (91) Li, Y.; Yang, J.; Aguilar, A.; McEachern, D.; Przybranowski, S.; Liu, L.; Yang, C.-Y.; Wang, M.; Han, X.; Wang, S. *J. Med. Chem.* **2019**, *62*, 448.
- (92) Smith, B. E.; Wang, S. L.; Jaime-Figueroa, S.; Harbin, A.; Wang, J.; Hamman, B. D.; Crews, C. M. *Nat. Commun.* **2019**, *10*, 1–13 (Article No. 131 (2019), DOI: 10.1038/s41467-018-08027-7).
- (93) Bassi, Z. I.; Fillmore, M. C.; Miah, A. H.; Chapman, T. D.; Maller, C.; Roberts, E. J.; Davis, L. C.; Lewis, D. E.; Galwey, N. W.; Waddington, K. E.; Parravicini, V.; Macmillan-Jones, A. L.; Gongora, C.; Humphreys, P. G.; Churcher, I.; Prinjha, R. K.; Tough, D. F. *ACS Chem. Biol.* **2018**, *13*, 2862.
- (94) Li, W.; Gao, C.; Zhao, L.; Yuan, Z.; Chen, Y.; Jiang, Y. *Eur. J. Med. Chem.* **2018**, *151*, 237.
- (95) Rubner, S.; Scharow, A.; Schubert, S.; Berg, T. *Angew. Chem., Int. Ed.* **2018**, *57*, 17043.
- (96) Han, T.; Goraliski, M.; Gaskill, N.; Capota, E.; Kim, J.; Ting, T. C.; Xie, Y.; Williams, N. S.; Nijhawan, D. *Science* **2017**, *356*, eaal3755 (DOI: 10.1126/science.aal3755).
- (97) Schiedel, M.; Herp, D.; Hammelmann, S.; Swyter, S.; Lehotzky, A.; Robaa, D.; Oláh, J.; Ovádi, J.; Sippl, W.; Jung, M. *J. Med. Chem.* **2018**, *61*, 482.
- (98) Xin, W.; Shaozhen, F.; Jinjin, F.; Xiaoyan, L.; Qiong, W.; Ning, L. *Biochem. Pharmacol.* **2016**, *116*, 200.
- (99) Ohoka, N.; Nagai, K.; Hattori, T.; Okuhira, K.; Shibata, N.; Cho, N.; Naito, M. *Cell Death Dis.* **2014**, *5*, e1513 (DOI:10.1038/cddis.2014.471).
- (100) Lu, M.; Liu, T.; Jiao, Q.; Ji, J.; Tao, M.; Liu, Y.; You, Q.; Jiang, Z. *Eur. J. Med. Chem.* **2018**, *146*, 251.
- (101) Chu, T.-T.; Gao, N.; Li, Q.-Q.; Chen, P.-G.; Yang, X.-F.; Chen, Y.-X.; Zhao, Y.-F.; Li, Y.-M. *Cell Chem. Biol.* **2016**, *23*, 453.
- (102) Crew, A. P.; Raina, K.; Dong, H.; Qian, Y.; Wang, J.; Vigil, D.; Serebrenik, Y. V.; Hamman, B. D.; Morgan, A.; Ferraro, C.; Siu, K.; Neklesa, T. K.; Winkler, J. D.; Coleman, K. G.; Crews, C. M. *J. Med. Chem.* **2018**, *61*, 583.
- (103) Maniaci, C.; Hughes, S. J.; Testa, A.; Chen, W.; Lamont, D. J.; Rocha, S.; Alessi, D. R.; Romeo, R.; Ciulli, A. *Nat. Commun.* **2017**, *8*, 1 (DOI: 10.1038/s41467-017-00954-1).
- (104) Montrose, K.; Krissansen, G. W. *Biochem. Biophys. Res. Commun.* **2014**, *453*, 735.
- (105) Cyrus, K.; Wehenkel, M.; Choi, E.-Y.; Han, H.-J.; Lee, H.; Swanson, H.; Kim, K.-B. *Mol. Biosyst.* **2011**, *7*, 359.
- (106) Nowak, R. P.; DeAngelo, S. L.; Buckley, D.; He, Z.; Donovan, K. A.; An, J.; Safaei, N.; Jedrychowski, M. P.; Ponthier, C. M.; Ishoe, M.; Zhang, T.; Mancias, J. D.; Gray, N. S.; Bradner, J. E.; Fischer, E. S. *Nat. Chem. Biol.* **2018**, *14*, 706.
- (107) Riching, K. M.; Mahan, S.; Corona, C. R.; McDougall, M.; Vasta, J. D.; Robers, M. B.; Urh, M.; Daniels, D. L. *ACS Chem. Biol.* **2018**, *13*, 2758.
- (108) Cromm, P. M.; Crews, C. M. *Cell Chem. Biol.* **2017**, *24*, 1181.
- (109) Savitski, M. M.; Zinn, N.; Faelth-Savitski, M.; Poeckel, D.; Gade, S.; Becher, I.; Muelbaier, M.; Wagner, A. J.; Strohm, K.; Werner, T.; Melchert, S.; Petretich, M.; Rutkowska, A.; Vappiani, J.; Franken, H.; Steidel, M.; Sweetman, G. M.; Gilan, O.; Lam, E. Y. N.; Dawson, M. A.; Prinjha, R. K.; Grandi, P.; Bergamini, G.; Bantscheff, M. *Cell* **2018**, *173*, 260.
- (110) Cong, L.; Ran, F. A.; Cox, D.; Lin, S.; Barretto, R.; Habib, N.; Hsu, P. D.; Wu, X.; Jiang, W.; Marraffini, L. A.; Zhang, F. *Science* **2013**, *339*, 819.
- (111) Jinek, M.; Chylinski, K.; Fonfara, I.; Hauer, M.; Doudna, J. A.; Charpentier, E. *Science* **2012**, *337*, 816.
- (112) Hall, M. P.; Unch, J.; Binkowski, B. F.; Valley, M. P.; Butler, B. L.; Wood, M. G.; Otto, P.; Zimmerman, K.; Vidugiris, G.; Machleidt, T.; Robers, M. B.; Benink, H. A.; Eggers, C. T.; Slater, M. R.; Meisenheimer, P. L.; Klaubert, D. H.; Fan, F.; Encell, L. P.; Wood, K. V. *ACS Chem. Biol.* **2012**, *7*, 1848.
- (113) Schwinn, M. K.; Machleidt, T.; Zimmerman, K.; Eggers, C. T.; Dixon, A. S.; Hurst, R.; Hall, M. P.; Encell, L. P.; Binkowski, B. F.; Wood, K. V. *ACS Chem. Biol.* **2018**, *13*, 467.
- (114) Machleidt, T.; Woodroffe, C. C.; Schwinn, M. K.; Méndez, J.; Robers, M. B.; Zimmerman, K.; Otto, P.; Daniels, D. L.; Kirkland, T. A.; Wood, K. V. *ACS Chem. Biol.* **2015**, *10*, 1797.
- (115) Hughes, S. J.; Ciulli, A. *Essays Biochem.* **2017**, *61*, 505.

Trademarks. HaloTag®, NanoBiT®, and NanoBRET® (Promega Corporation).

About the Authors


Sarah Schlesiger studied chemistry in Germany, France, and Australia, earning an M.Sc. degree from Leipzig University (2012). She completed her Ph.D. dissertation (2017) in chemical biology at the University of Konstanz working with Professor Dr. Andreas Marx. Shortly thereafter, Sarah joined

Merck KGaA, Darmstadt, Germany, and is currently working as Laboratory Head in medicinal chemistry seeking to develop tomorrow's medicines.

Momar Toure studied chemistry at ENSCM, France, where he earned his M.Sc. degree in 2010. He then completed the requirements for his Ph.D. degree in 2013 in the research group of Drs. Jean-Luc Parrain and Olivier Chuzel at Aix-Marseille University, France. He then joined Professor Craig Crews's research group at Yale University, where he worked in the PROTAC field. He is currently Senior Research Scientist at EMD Serono.

Kaelyn E. Wilke studied biochemistry at the University

of St. Thomas, St. Paul, Minnesota, and completed the requirements for her Ph.D. degree in chemical biology with Professor Erin Carlson at Indiana University. Kaelyn joined the Chemical Synthesis Group at MilliporeSigma in 2015, where she is currently Product Manager developing and commercializing technology within emerging areas of chemical biology and medicinal chemistry.

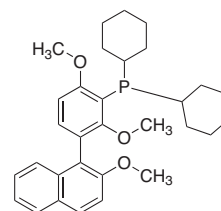
Bayard R. Huck received his Ph.D. degree in organic chemistry from the University of Wisconsin-Madison under the direction of Professor Samuel H. Gellman. He is currently the Global Head of Medicinal Chemistry at Merck KGaA, Darmstadt, Germany. 

PRODUCT HIGHLIGHT

Explore further with New Chemical Synthesis Products

Our goal is to drive your research forward by bringing the latest compounds in the literature to a bottle.

EvanPhos (**902292**) is a new biaryl phosphine ligand designed in the laboratory of Professor Lipshutz for use in Suzuki-Miyaura cross couplings in conjunction with a Pd(0) source. EvanPhos can be used in either organic solvents or under aqueous micellar conditions with the surfactant TPGS-750-M (**733857**) making this an attractive technology for greener chemistry.



902292

To view these and other new products, visit
[SigmaAldrich.com/newchemistry](https://www.sigmaaldrich.com/newchemistry)

Get connected

Get ChemNews

Get current news and information about chemistry with our free monthly *ChemNews* email newsletter. Learn new techniques, find out about late-breaking innovations from our collaborators, access useful technology spotlights, and share practical tips to keep your lab at the fore.

For more information, visit
SigmaAldrich.com/ChemNews



The life science
business of Merck
operates as
MilliporeSigma in the
U.S. and Canada.

Sigma-Aldrich®
Lab & Production Materials

Coumarin-Based Hybrids as Fluorescent Probes for Highly Selective Chemosensing and Biological Target Imaging



Dr. C. S. Francisco



Ms. T. C. Valim



Prof. Dr. Á. C. Neto



Prof. Dr. V. Lacerda, Jr.

Carla Santana Francisco, Thays Cardoso Valim, Álvaro Cunha Neto, and Valdemar Lacerda, Jr.*

Department of Chemistry
Center of Exact Sciences
Federal University of Espírito Santo,
Goiabeiras Campus
Fernando Ferrari Avenue, 514
Goiabeiras, Vitória, ES 29075-910, Brazil
Email: vljuniorqui@gmail.com

Keywords. coumarins; coumarin hybrids; chemosensors; fluorescent probes; chromogenic dyes; fluorogenic dyes; biological target imaging; fluorescent sensors; molecular recognition; biological sensors.

Abstract. The coumarins are considered an attractive compound class because the coumarin nucleus is an important, biologically active pharmacophore that plays a significant role in chemical biology and in medical applications. Moreover, due to their excellent photophysical properties, coumarins constitute an important class of chromogenic and fluorogenic dyes. In this article, we review a wide range of very recently reported applications of coumarin hybrids as chemosensors, fluorescent probes, biological markers, and biological trackers.

Outline

1. Introduction
2. Synthetic Methods for the Preparation of Coumarin-Based Hybrids
3. Applications of Coumarin Hybrids as Fluorescent Probes for Chemosensing and Target Imaging
 - 3.1. Detection of Mercury(II)
 - 3.2. Detection of Copper(II)
 - 3.3. Ratiometric Sensing of Zinc(II)
 - 3.4. Chemosensing of Aluminum(III), Phosphate, and Pyrophosphate
 - 3.5. Ratiometric Fluorescence Detection of Fluoride
 - 3.6. Sensing of Hypochlorite (ClO⁻) in Aqueous Media and Living Cells
 - 3.7. Colorimetric and Ratiometric Detection of Sulfite
 - 3.8. Hydrogen Peroxide Detection
 - 3.9. Biothiol Detection and Imaging
4. Conclusion
5. Acknowledgments
6. References

1. Introduction

Coumarin is a privileged scaffold, owing to its characteristic structure in which a planar aromatic ring is fused to a lactone functionality and to its conjugated π system, fluorescent properties, and other desirable features. This framework has attracted the attention of several research groups, who incorporated the coumarin scaffold into heterocyclic and non-heterocyclic systems as part of a strategy for obtaining hybrid molecules with potentially versatile biological activities, better selectivity profiles, different or double modes of action, and/or reduced undesirable side effects (**Figure 1**).¹

Fluorescent probes are considered crucial tools for molecular recognition events in biological systems.² In recent years, a number of fluorescent probes have been developed, which possess desirable properties such as high selectivity and sensitivity, straightforward implementation, and noninvasive in situ detection. Among these, coumarin-hybrid probes have been widely utilized in tumor diagnosis or in analyte target detection, enzymes, and organelles. Coumarin dyes are often selected because of their good water solubility, strong fluorescence, relatively high fluorescence quantum yield, and facile synthesis.³

In the remainder of this review, we highlight recently reported new molecules that incorporate coumarin rings, with the aim of contributing an understanding that would permit the discovery of novel compounds with improved properties for application as chemosensors and fluorescent probes.

2. Synthetic Methods for the Preparation of Coumarin-Based Hybrids

Generally, molecular systems incorporating a coumarin moiety and intended for biological, pharmaceutical, and biomedical applications have been assembled using traditional synthetic chemistry. This includes classical transformations such as the Perkin, Wittig, and Reformatsky reactions; the Pechmann and Knoevenagel condensations; and the Claisen rearrangement. An example of such methods is the use of the Pechmann condensation in the straightforward synthesis of the new fluorescent chemodosimeter **1**, incorporating a coumarin fluorophore and a carbonothiolate functionality as the recognition unit (Scheme 1).⁴ Compound **1** was then used for the detection of Hg²⁺ concentrations in real water samples by fluorescence turn-on response. The Pechman condensation, however, suffers in general from a number of drawbacks such as the need for excess acid and the production under some circumstances of byproducts such as chromone.⁵

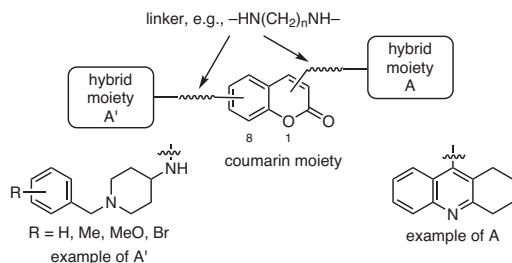
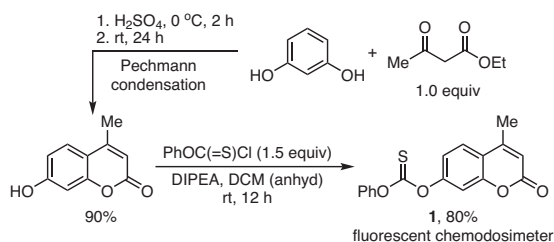


Figure 1. General Structure of a Coumarin-Hybrid Pharmacophore. (Ref. 1)



Scheme 1. An Example of the Use of the Pechmann Condensation as a Key Step in the Synthesis of the New Fluorescent Chemodosimeter **1**. (Ref. 4)

The Knoevenagel condensation is also extensively used for the synthesis of coumarin scaffolds, which are later incorporated into other small molecules of interest in chemistry and biology.^{6–17} This reaction can be catalyzed by piperidine, piperazine, 1,1'-carbonyldiimidazole (CDI), 1,8-diazabicyclo[5.4.0]undec-7-ene (DBU), or an ionic liquid, among others.¹⁸ An example of its utilization in the synthesis of a dual-emission ratiometric fluorescent chemosensor, **2**, with applications in cellular imaging is depicted in Scheme 2.⁶

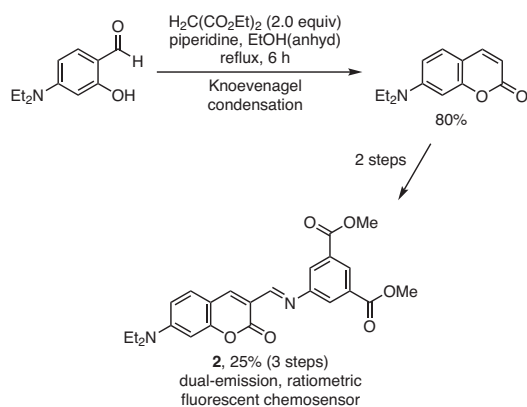
In addition to these popular traditional methods, other approaches have been explored for the purpose of enhancing yields, reducing reaction times, and improving product recovery.¹⁹ These include reactions that use microwave irradiation, sonication, transition-metal catalysis, heterogeneous catalysis, or ionic liquids.

3. Applications of Coumarin Hybrids as Fluorescent Probes for Chemosensing and Target Imaging

Because of their easy operating techniques, real-time response, and high selectivity and sensitivity, fluorescent chemical sensors have been developed in recent years as powerful tools for monitoring levels of ions, molecules, and other chemical entities. In particular, coumarin-based compounds are attractive as fluorescent sensors because of their excellent chromogenic and fluorogenic properties, associated high quantum yields, excellent water solubility, large Stokes relative displacement, and good cell permeability.²⁰ Moreover, and owing to their highly variable size, hydrophobicity, and chelation capabilities, coumarin-based hybrids have found specific applications as highly selective fluorescent probes for detecting metal ions.²¹

3.1. Detection of Mercury(II)

Because of the serious risk that mercury in the environment poses to human health and biological reproduction, the development of mercury detection probes has gained in prominence in recent

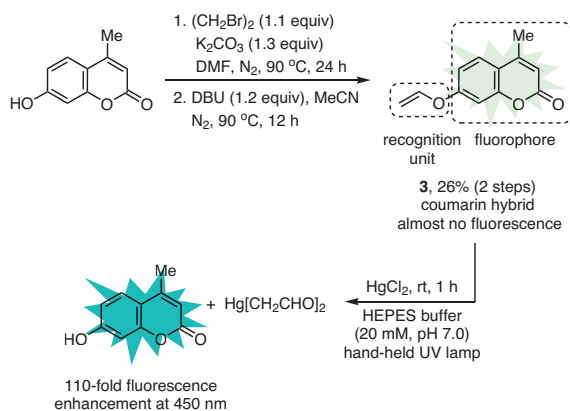


Scheme 2. An Example of the Use of the Knoevenagel Condensation as a Key Step in the Synthesis of the Dual-Emission Ratiometric Fluorescent Chemosensor **2**. (Ref. 6)

years.²² Relevant studies can be performed in water, in another solvent when water solubility is low, and even in a range of pH values for those probes that are not sensitive to pH.

7-Vinyloxy-4-methylcoumarin (**3**), a hybrid comprising methylcoumarin as a fluorophore and a vinyl ether group as a recognition unit, was shown to be highly selective and sensitive to Hg^{2+} in aqueous solutions (Scheme 3).²³ Wang, Zhou, and co-workers pointed out that, when compared to other systems, the protocol they developed using **3** is a low cost, simple, and highly sensitive Hg^{2+} detection method. Similarly, coumarin dye hybrid **2** (see Scheme 2) was employed by Jiao et al. as a highly selective, ratiometric fluorescent chemosensor to detect nanomolar levels of Hg^{2+} at physiological pH.⁶ Interestingly, the novel, rectilinear, and π -extended rhodol-coumarin hybrid dye **4** was shown to possess high selectivity for Hg^{2+} ions on a nanomolar scale, even in the presence of biologically or environmentally relevant alkali, alkaline earth, and transition metal ions (Scheme 4).²⁴ The detection mechanism is believed to involve an Hg^{2+} -promoted reaction cascade consisting of ring-opening and desulfurization. Moreover, incubation of **4** with HeLa cells [37 °C, 1.5 h, CO_2 atmosphere (5%)] with and without Hg^{2+} suggested that **4** is living-cell-membrane permeable, making it suitable for practical in vitro applications.

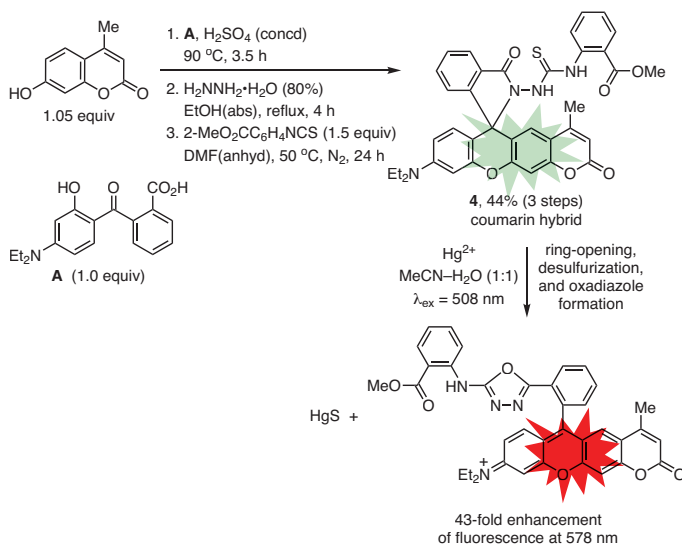
Cheng and co-workers have recently reported the synthesis of a pair of novel and water-soluble thioacetalized coumarin hybrids and their application as ratiometric fluorescent probes that are highly selective for Hg^{2+} ions. The chemosensing ability was attributed to the mercury(II)-promoted conversion reaction of the dithioacetal functional group into the corresponding aldehyde with a corresponding shift in fluorescence from blue to green visible with the naked eye (Scheme 5).²² The authors also showed that coumarin-hybrid probe **5** penetrates the membrane of HeLa cells and could potentially be used for the fluorescent imaging of mercury(II) in living cells.



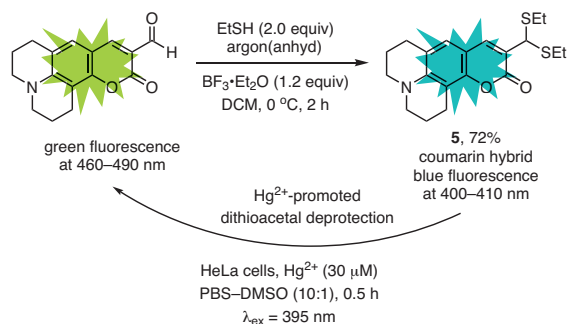
Scheme 3. Synthesis and Testing of 7-Vinyloxy-4-methylcoumarin (**3**) as a Coumarin-Hybrid Fluorescent Probe with High Selectivity for Mercuric Ion. (Ref. 23)

3.2. Detection of Copper(II)

Cupric ion plays a key role in several basic physiological processes, and is the third most abundant heavy metal in humans. However, high levels of copper(II) in the human body can cause oxidative stress and disorders associated with neurodegenerative diseases, as well as rheumatoid arthritis, gastrointestinal disturbances, and Wilson's disease; in the environment, Cu^{2+} is considered a pollutant that is potentially very harmful to organisms.^{7,21} A novel, highly selective, and highly sensitive method for detecting Cu^{2+} in acetonitrile in the presence of other metal ions has been reported by Mei, Zhou, and co-workers. This approach relies on colorimetric and fluorescence changes that result from a Cu^{2+} -induced intramolecular nucleophilic addition in coumarin-hybrid **6**, leading to a substituted imidazole ring (Scheme 6).⁷ The changes, which are complete in less than 3



Scheme 4. Novel and Living-Cell-Membrane Permeable Rhodol-Coumarin Hybrid Dye **4** with Potential in Vitro Applications. (Ref. 24)



Scheme 5. Dithioacetal-Functionalized Coumarin-Based Probe for the Bioimaging of Mercury(II) in HeLa Cells. (Ref. 22)

minutes, would allow this process to be utilized for the real-time tracking of copper(II). The authors were also able to extend this methodology to detecting intracellular copper(II) in HepG2 cells, thus demonstrating that compound **6** could be employed as a practical and reliable probe for imaging Cu^{2+} in living cells.

The monitoring of Hg^{2+} and Cu^{2+} in the mitochondria of HeLa cells and mouse kidney tissues using the two new, structurally related, coumarin-based, and biocompatible fluorescent sensors **7** and **8** has been described by Zhou and co-workers (Scheme 7).²⁵ The authors carried out bioimaging experiments, fluorescence co-localization studies, and time effects studies in vitro to evaluate the ligands' response to metal ions. Both probes exhibited excellent selectivity for mercury(II) and copper(II) even in the presence of other ions. Probe **7** exhibited

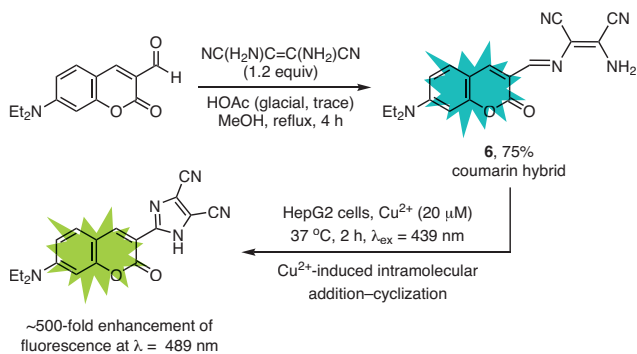
an excellent selective fluorescence response to Hg^{2+} in $\text{MeOH-H}_2\text{O}$, whereby its fluorescence intensity increased significantly for Hg^{2+} but changed only slightly in the presence of Cu^{2+} . In contrast, probe **8** exhibited significantly increased fluorescence intensity upon addition of Hg^{2+} but complete attenuation of fluorescence upon addition of Cu^{2+} in H_2O .

A number of other novel, coumarin-based fluorescent probes have also been developed and successfully tested for the selective detection of copper(II) under a variety of experimental conditions and in living cells (Figure 2).^{8,9,21,26} In these cases, Cu^{2+} induces fluorescence enhancement or quenching either through complexation with the probe or through initial complexation followed by hydrolysis of an imino group to generate the fluorescent species.

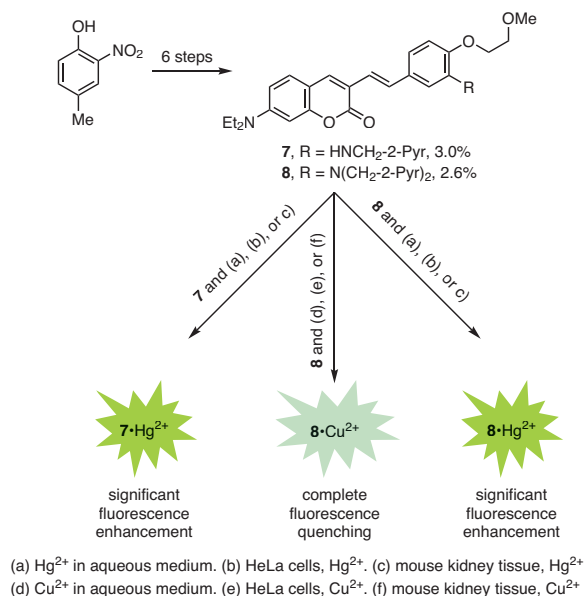
3.3. Ratiometric Sensing of Zinc(II)

Zinc is one of the most important transition metals. It is present in the human body in nanomolar (nM) to millimolar (mM) concentrations, and is involved in a variety of biological processes. Genetic abnormalities and environmental factors may lead to disturbances in the metabolism of zinc, resulting in a variety of diseases such as Alzheimer's disease, Parkinson's disease, epilepsy, cerebral ischemia, amyotrophic lateral sclerosis (ALS), diabetes, and childhood diarrhea. As a consequence, there is keen interest in developing suitable fluorescent probes for detecting Zn^{2+} in order to help maintain its physiological concentrations at suitable levels.

To this end, two new, coumarin-based ligands, **9a** and **9b**, have been synthesized and evaluated as ratiometric fluorescent



Scheme 6. Coumarin-Based Fluorescence Off-On Probe for Detecting Intra- and Extracellular Copper(II). (Ref. 7)



Scheme 7. New, Structurally Related Fluorescent Probes That Are Highly Selective for Hg^{2+} and Cu^{2+} in Vitro, in HeLa Cells, and in Mouse Kidney Tissues. (Ref. 25)

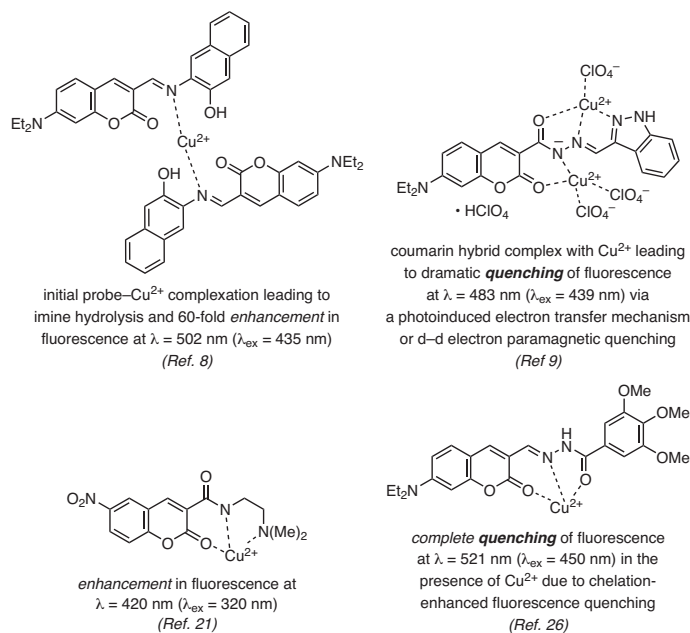


Figure 2. Novel Coumarin-Hybrid Chemosensors of Copper(II) Either via Enhancement or Quenching of Fluorescence.

probes for detecting and quantifying Zn^{2+} in aqueous media and in living cells (**Figure 3**).^{10,11} Both displayed good selectivity and high sensitivity toward Zn^{2+} without interference by other metal ions, especially by Cd^{2+} , which is in the same periodic table group as Zn^{2+} . For both **9a** and **9b**, the ratiometric fluorescence response was ascribed to enhanced intramolecular charge-transfer upon binding of the ligand to Zn^{2+} . In ethanol-water (9:1), coumarin-furan hybrid, **9a**, exhibited a fast (0.5 min) and reversible ratiometric fluorescence response, suggesting that **9a** could be employed as a ratiometric fluorescent sensor for the detection and monitoring of Zn^{2+} in environmental and biological systems in real time and under physiological conditions.¹⁰ Similarly, coumarin-quinoline hybrid **9b** showed significant colorimetric and ratiometric responses to Zn^{2+} , exhibited low toxicity, and had good cell-membrane permeability at physiological temperature in MCF-7 cells.¹¹ It was also suggested that **9b** could be utilized for the qualitative determination of Zn^{2+} in living cells and its quantitative detection in environmental water samples.

3.4. Chemosensing of Aluminum(III), Phosphate, and Pyrophosphate

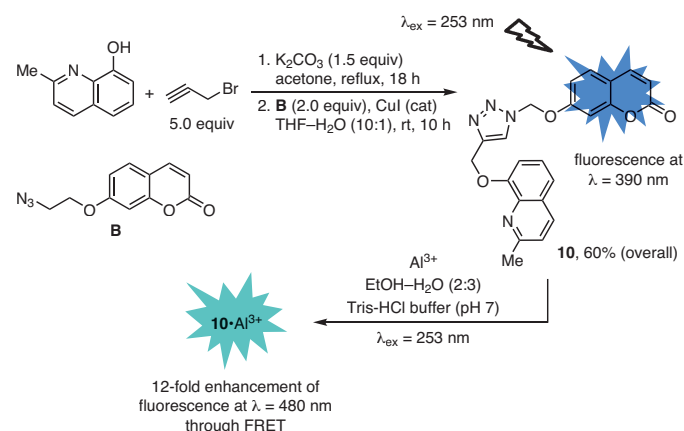
Two modes of fluorescence enhancement have been employed for the selective and highly sensitive detection of aluminum(III) in aqueous buffers at neutral pH values in the presence of other metal ions and its bioimaging in living cells (HeLa or PC3). The first mode relies on an Al^{3+} -triggered fluorescence resonance energy transfer (FRET) from quinoline to coumarin in the ratiometric fluorescent small-molecule probe **10** (**Scheme 8**).²⁷ This chemosensor had a very low detection limit for Al^{3+} (1×10^{-6} M) and passed through HeLa or PC3 cell membranes in a short period of time, making it suitable for monitoring intracellular aluminum(III) in vitro and potentially in vivo.

In the second mode, chelation-enhanced fluorescence (CHEF) was taken advantage of in developing a highly sensitive and selective coumarin-Schiff base sensor, **11**, for detecting Al^{3+} in 90% aqueous methanol at pH 7.4 (HEPES buffer) and

in living HeLa cells (**Scheme 9**).²⁸ The 1:1 complex resulting from the binding of Al^{3+} to **11** was found to act by the reverse process, fluorescence attenuation, as a highly selective probe for detecting pyrophosphate (HP_2O_7^-) and phosphate (H_2PO_4^-) anions, such as found in calf thymus DNA (ctDNA), in the presence of 20 equivalents of other competitive anions such as acetate and nitrate.

3.5. Ratiometric Fluorescence Detection of Fluoride

A new, silyl-protected fluorescein-coumarin hybrid, **12**, has been reported by Ma, Song, and co-workers as a highly selective and sensitive probe for the ratiometric fluorescence detection of fluoride ion in the presence of other competing anions, reactive oxygen species (e.g., H_2O_2 , ClO^- , ONOO^-), and sulfur-containing organics (e.g., GSH, Cys).¹² Upon addition of F^- ,



Scheme 8. Chemosensing of Al^{3+} via a Fluorescence Resonance Energy Transfer (FRET) Mechanism. (Ref. 27)

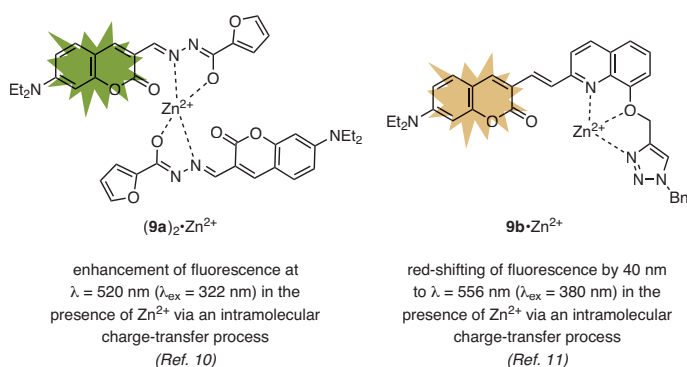
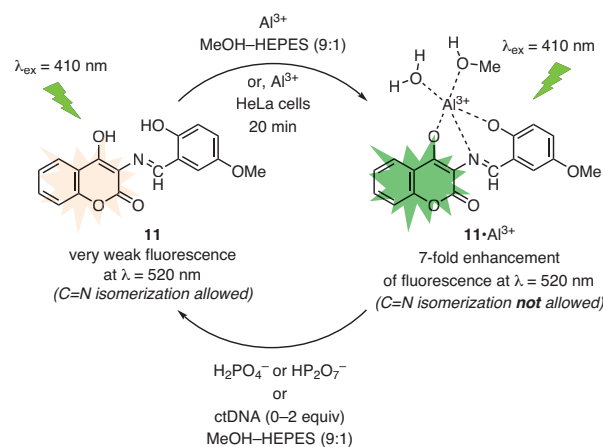


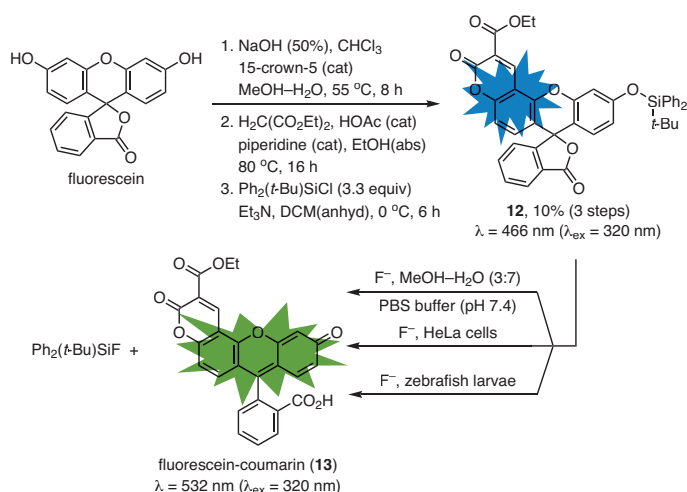
Figure 3. Ratiometric Fluorescent Sensors Suitable for the Detection and Monitoring of Zinc(II) in Environmental and Biological Systems.



Scheme 9. Coumarin-Schiff Base Probe for the Highly Selective Detection of Aluminum(III) as Well as Pyrophosphate and Phosphate Anions in the Presence of Competing Ions. (Ref. 28)

desilylation of the phenolic oxygen occurs by rapid reaction of fluoride with the *tert*-butyldiphenylsilyl (TBDPS) protecting group leading to fluorescein-coumarin hybrid **13**, and a change of fluorescence from blue to green (**Scheme 10**). The limit of detection (LOD) for fluoride was calculated to be $0.025 \mu\text{M}$, and the process was successfully applied to the bioimaging of fluoride in living HeLa cells and 5-day-old zebrafish larvae, hinting at the potential application of this process in clinical diagnosis. Another coumarin-based, ratiometric fluorescent probe that relies on a desilylation of a triisopropylsilyl group by fluoride ion was reported by Shen et al., and successfully applied to the detection of fluoride in mitochondria of living HepG2 cells by ratiometric fluorescence imaging.²⁹

Two other effective and highly selective sensors for fluoride ion have also been reported. These rely on fast colorimetric changes or fluorescence quenching to selectively detect and determine fluoride ion concentration (**Figure 4**).^{13,14} They also proved to have high response rates and very low fluoride detection limits (e.g., $\text{LOD} = 2.16 \times 10^{-7} \text{ M}$).



Scheme 10. Highly Selective and Sensitive Ratiometric Fluorescence Detection and Quantification of Fluoride Ion Based on Its Well-Known Affinity for the *tert*-Butyldiphenylsilyl Group. (Ref. 12)

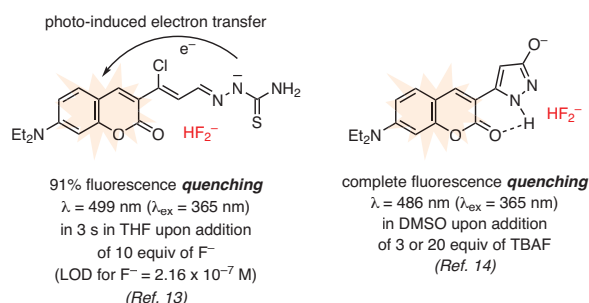
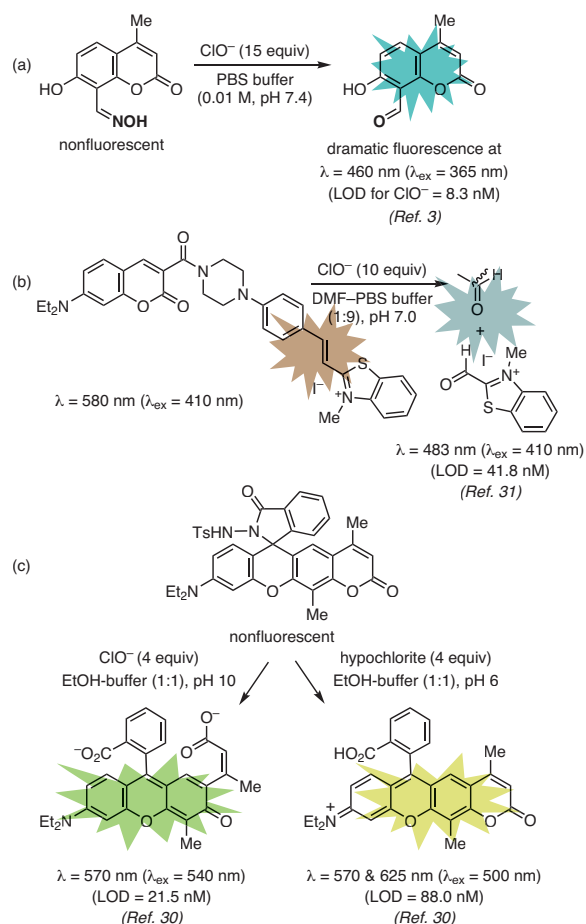


Figure 4. Other Effective and Highly Selective Coumarin-Based Sensors for Fluoride Ion.

3.6. Sensing of Hypochlorite (ClO^-) in Aqueous Media and Living Cells

Hypochlorous acid and its conjugated base (HClO/ClO^-) play an important role in biological systems; however, excessive production of HClO/ClO^- could lead to several types of disorders, such as Parkinson's disease, rheumatism, lung injury, arthritis, degeneration of neurons, and even certain cancers. Hence, the monitoring of hypochlorite anion (ClO^-) in a sensitive and selective manner in aqueous media and living cells is of great interest.

To this end, a number of research groups have reported highly sensitive and selective coumarin-based hybrids for the ratiometric fluorescence detection of hypochlorite in water samples and in mitochondria of living cells (**Scheme 11**).^{3,30,31} Rapid response times (e.g., 20–30 s) and low detection limits (e.g., 8.3–22 nM) were observed with these probes, without interference by other anions or reactive oxygen or nitrogen species (e.g., HO^\bullet , H_2O_2 , $\text{O}_2^{\bullet-}$, $^1\text{O}_2$, $t\text{-BuO}^\bullet$, ONOO^- , NO^\bullet , NO_2^-) over a range of pH values. The hypochlorite-recognition mechanism of these probes relied in each case on a unique chemical reaction triggered by ClO^- —such as oxime oxidation to an aldehyde, δ -lactone ring-opening,



Scheme 11. Selective ClO^- Detection by Hypochlorite-Triggered Unique Reactivity of Coumarin-Based Fluorescent Probes.

or oxidative cleavage of a carbon–carbon double into two formyl groups—and resulting in an intense fluorescence response. The probes were successfully applied to the determination of ClO^- in real water samples (tap, river, and lake water, as well as diluted commercial disinfectant) and to the bioimaging of hypochlorite in RAW264.7 and SW480 cells.

3.7. Colorimetric and Ratiometric Detection of Sulfite

Endogenous sulfur dioxide (SO_2) is present in mammalian cells in the form of its aqueous derivatives (HO_3S^- and SO_3^{2-}), which are generated in biosynthetic pathways from sulfur-containing amino acids through the action of enzymes such as thiosulfate sulfurtransferase. While low concentrations of sulfites can be beneficial, abnormally high concentrations are associated with a number of health disorders such as respiratory and cardiovascular diseases.^{15,32} Moreover, sulfur dioxide is a recognized air pollutant generated by the burning of fossil fuels. The detection, determination, and monitoring of the levels of SO_2 and its derivatives in the environment and in biological systems is therefore of great interest.

The research groups of Qian,¹⁵ Zhao,³² and Wang³³ have independently developed coumarin hybrids for sensing sulfites in aqueous media and living cells, such as human colon cancer cells SW480 as well as HeLa, HepG2, L-02, and L929 cells (Figure 5). Highly selective, sensitive, and rapid colorimetric, ratiometric, or turn-on fluorescence sensing was achieved in each case with sulfite detection limits in the nano- to micromolar range. The sensing mechanisms consisted of either a disruption of π conjugation via bisulfite addition to a double bond,¹⁵ SO_3^{2-} -addition to a hemicyanine moiety that interrupts an ICT/FRET process,³² or the liberation of 6-hydroxycoumarin from its levulinic ester precursor.³³

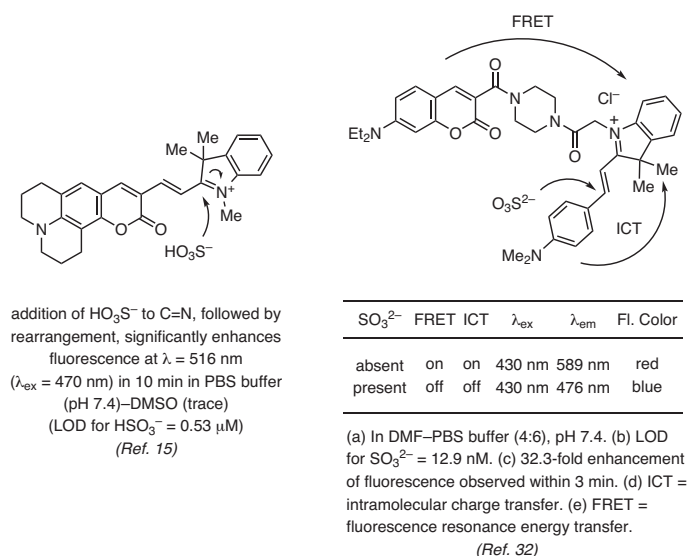


Figure 5. Rapid, Selective, and Sensitive Detection of Sulfur Dioxide Derivatives.

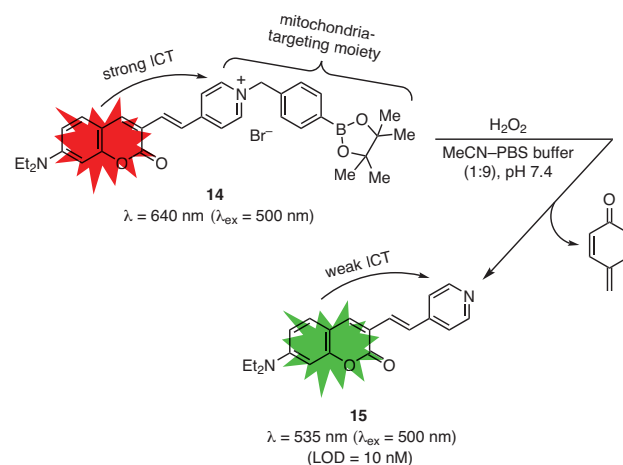
3.8. Hydrogen Peroxide Detection

The known reactivity of hydrogen peroxide toward boronates has been taken advantage of in the design and testing of new coumarin-based probes for the detection of hydrogen peroxide in aqueous buffer and in mitochondria of living cells.^{34,35} In one instance, Shen et al. have demonstrated that coumarin–pyridinium hybrid **14** can be utilized as a highly sensitive and selective colorimetric and ratiometric fluorescent sensor for H_2O_2 with an LOD of 10 nM (eq 1).³⁵ They also showed that this probe is not responsive to other biologically relevant reactive oxygen species (ROS), reactive nitrogen species (RNS), or metal ions, as these did not cause any significant change in the I_{535}/I_{640} emission ratio under the same conditions. Additionally, the authors reported the successful application of this probe to the bioimaging of hydrogen peroxide in mitochondria of NRK cells with a response time of 5 minutes. Investigation of the sensing mechanism by ^1H NMR and HRMS as well as by density functional theory (DFT) calculations revealed that it takes place through oxidation of the boronate with hydrogen peroxide followed by hydrolysis and 1,6-elimination to form coumarin–pyridine **15**.

3.9. Biothiol Detection and Imaging

Thiol-containing biomolecules, known collectively as biothiols, include cysteine (Cys) and homocysteine (Hcy) amino acids and the low-molecular-weight antioxidant peptide glutathione (GSH). Biothiols play important roles in biological systems, and their levels within cells or in human plasma are indicative of underlying disorders and risk factors for a broad range of conditions and diseases.³⁶ It is thus not surprising that the development of effective fluorescent probes for the selective detection of specific biothiols has been an active area of research aiming to provide tools and methods for the early diagnosis of these conditions, risk factors, and disorders.^{37–43}

Among the effective biothiol sensors developed, coumarin derivative **16** proved to be a highly sensitive colorimetric and fluorescent probe not only for the imaging of cysteine and



eq 1 (Ref. 35)

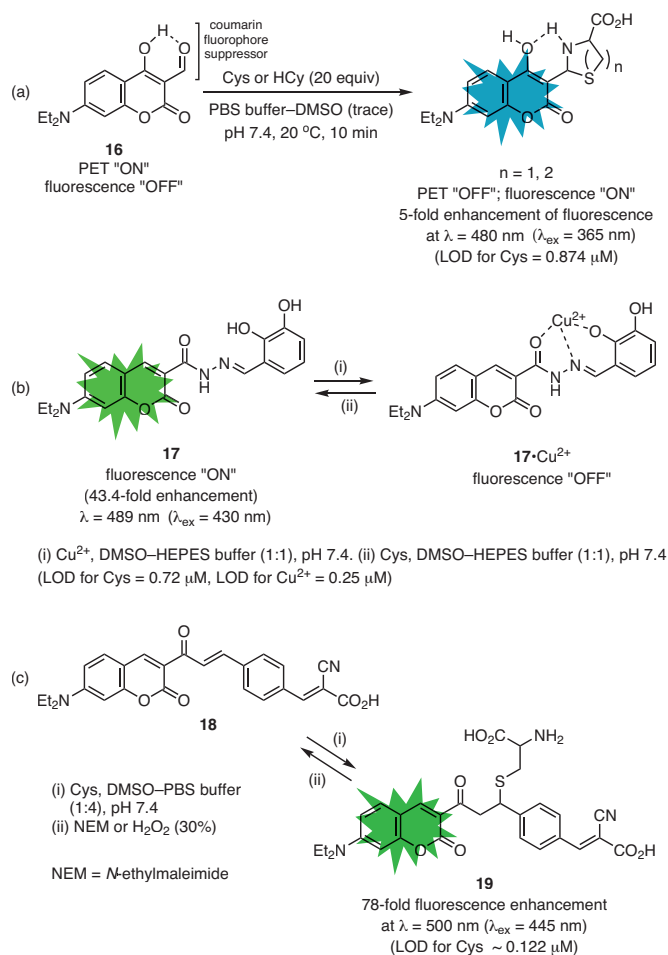
homocysteine over GSH in living HeLa cells and mouse liver tissue, but also for their detection in five types of animal serum from chicken, horse, sheep, cattle, and goat. This rapid and biocompatible probe works by fluorescence turn-on following suppression of a photoinduced electron transfer (PET) as a result of a cyclization reaction between the thiol group and the aldehyde functional group in the probe, and was not responsive to 19 other amino acids tested (Scheme 12, Part (a)).³⁶

Meng et al. reported another new and effective coumarin-based chemosensor, **17**, for cysteine in buffer solution, in the endoplasmic reticulum of live U-343 MGa and MDA-MB-231 cells, and in real urine samples. Probe **17** achieves the highly selective and sensitive detection of Cys (LOD for Cys = 0.72 μM) through an “ON-OFF-ON” fluorescence process (Scheme 12, Part (b)).³⁸ In the absence of copper(II), **17** is highly fluorescent; this fluorescence is significantly reduced (98.4% quenching) after addition of Cu^{2+} , which forms a complex with **17**. However, upon incubation with Cys, complex **17**· Cu^{2+} is decomposed, and highly fluorescent **17** is released with 43.4-fold enhancement in

fluorescence that is not affected by the presence of competing biomolecules and physiologically important anions.

Yin, Huo, and co-workers reported the first recyclable coumarin-based sensor, **18**, for the rapid turn-on fluorescence detection of Cys in aqueous buffer and exogenous Cys in living A549 and Hela cells (Scheme 12, Part (c)).⁴² Probe **18** showed a 78-fold fluorescence enhancement upon addition of Cys—by forming the cysteine thiol 1,4-addition product, **19**—and could detect Cys even in the presence of biothiols Hcy and GSH, common amino acids, metal ions, physiologically relevant anions, *N*-acetylcysteine, and H_2O_2 . The specificity of the response of **18** toward Cys was demonstrated in an “ON-OFF-ON” fluorescence sequence, whereby the quenching effects of *N*-ethylmaleimide (NEM) or H_2O_2 on the fluorescence of **19** were reversed by re-introducing Cys. The authors subjected probe **18** to five such “ON-OFF-ON” cycles and observed no noticeable attenuation in the fluorescence of **19**, providing evidence for the recyclability of **18**.

A number of other, novel, and coumarin-based probes have been synthesized and successfully utilized for the highly selective fluorescent sensing of biothiols such as cysteine, homocysteine, and glutathione in aqueous buffer and in living cells without interference by other physiologically relevant molecular species or anions (Figure 6).^{16,37,39–41,43} However, the limits of detection of these probes for biothiols varied widely from 0.46 nM to 657 nM (Cys), 0.86 to 79 nM (Hcy), and 0.73 nM to 1.07 μM (GSH). In one case, the coumarin-based probe proved effective also for detecting cyanide ion (LOD for CN^- = 0.32 nM).⁴⁰



Scheme 12. Examples of Highly Selective and Sensitive Fluorescent Probes for the Determination of Biothiols. (Ref. 36,38,42)

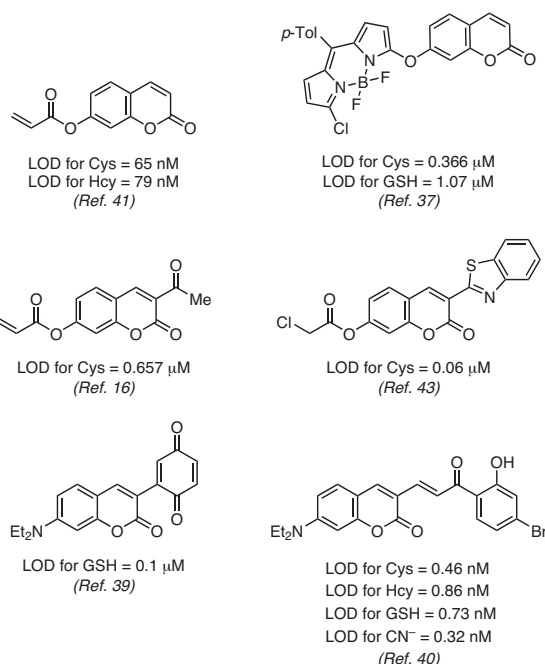


Figure 6. Additional, Selective, and Sensitive Coumarin-Based Sensors for the Detection and Imaging of Biothiols.

4. Conclusion

We have highlighted in this review the rapidly growing applications of coumarin–small-molecule hybrids as fast and highly selective and sensitive fluorescent probes for detecting, quantifying, and bioimaging of a wide variety of physiologically relevant metal ions, anions, molecules, reactive oxygen species, and reactive nitrogen species. It is our sincere hope that the review will prove of great benefit to a wide range of researchers looking to capitalize on ever more sensitive and selective tools for the assay of analytes of interest in biological systems.

5. Acknowledgments

The authors thank the National Council for Scientific and Technological Development (CNPq), the Coordination Bureau for the Improvement of Higher Education Personnel (CAPES), and the Espírito Santo Research Foundation (FAPES) for financial support and fellowships.

6. References

- Ibrar, A.; Shehzadi, S. A.; Saeed, F.; Khan, I. *Bioorg. Med. Chem.* **2018**, *26*, 3731.
- Fu, Y.-J.; Yao, H.-W.; Zhu, X.-Y.; Guo, X.-F.; Wang, H. *Anal. Chim. Acta* **2017**, *994*, 1.
- Han, J.; Li, Y.; Wang, Y.; Bao, X.; Wang, L.; Ren, L.; Ni, L.; Li, C. *Sens. Actuators, B* **2018**, *273*, 778.
- Li, Q.; Hu, Y.; Hou, H.-N.; Yang, W.-N.; Hu, S.-L. *Inorg. Chim. Acta* **2018**, *471*, 705, and reference 24 therein.
- Choi, H.; Kim, J.; Lee, K. *Tetrahedron Lett.* **2016**, *57*, 3600.
- Jiao, Y.; Liu, X.; Zhou, L.; He, H.; Zhou, P.; Duan, C. *Sens. Actuators, B* **2017**, *247*, 950.
- Yang, M.; Wang, H.; Huang, J.; Fang, M.; Mei, B.; Zhou, H.; Wu, J.; Tian, Y. *Sens. Actuators, B* **2014**, *204*, 710.
- Wang, S.; Wang, Z.; Yin, Y.; Luo, J.; Kong, L. *J. Photochem. Photobiol., A* **2017**, *333*, 213.
- He, G.; Liu, X.; Xu, J.; Ji, L.; Yang, L.; Fan, A.; Wang, S.; Wang, Q. *Spectrochim. Acta, Part A* **2018**, *190*, 116.
- Li, C.; Li, S.; Yang, Z. *Spectrochim. Acta, Part A* **2017**, *174*, 214.
- Wu, G.; Gao, Q.; Li, M.; Tang, X.; Lai, K. W. C.; Tong, Q. *J. Photochem. Photobiol., A* **2018**, *355*, 487.
- Jiao, S.; Wang, X.; Sun, Y.; Zhang, L.; Sun, W.; Sun, Y.; Wang, X.; Ma, P.; Song, D. *Sens. Actuators, B* **2018**, *262*, 188.
- Ma, L.; Leng, T.; Wang, K.; Wang, C.; Shen, Y.; Zhu, W. *Tetrahedron* **2017**, *73*, 1306.
- Babür, B.; Seferoğlu, N.; Seferoğlu, Z. *J. Mol. Struct.* **2018**, *1161*, 218.
- Yao, Y.; Sun, Q.; Chen, Z.; Huang, R.; Zhang, W.; Qian, J. *Talanta* **2018**, *189*, 429.
- Dai, X.; Wu, Q.-H.; Wang, P.-C.; Tian, J.; Xu, Y.; Wang, S.-Q.; Miao, J.-Y.; Zhao, B.-X. *Biosens. Bioelectron.* **2014**, *59*, 35.
- Liao, Y.-C.; Venkatesan, P.; Wei, L.-F.; Wu, S.-P. *Sens. Actuators, B* **2016**, *232*, 732.
- Vekariya, R. H.; Patel, H. D. *Synth. Commun.* **2014**, *44*, 2756.
- Priyanka; Sharma, R. K.; Katiyar, D. *Synthesis* **2016**, *48*, 2303.
- Li, J.; Zhang, C.; Wu, S.; Wen, X.; Xi, Z.; Yi, L. *Dyes Pigm.* **2018**, *151*, 303.
- Bekhradnia, A.; Domehri, E.; Khosravi, M. *Spectrochim. Acta, Part A* **2016**, *152*, 18.
- Cheng, X.; Qu, S.; Xiao, L.; Li, W.; He, P. *J. Photochem. Photobiol., A* **2018**, *364*, 503.
- Wu, C.; Wang, J.; Shen, J.; Bi, C.; Zhou, H. *Sens. Actuators, B* **2017**, *243*, 678.
- Huang, K.; Jiao, X.; Liu, C.; Wang, Q.; Qiu, X.; Zheng, D.; He, S.; Zhao, L.; Zeng, X. *Dyes Pigm.* **2017**, *142*, 437.
- Yao, S.; Zhang, G.; Wang, H.; Song, J.; Liu, T.; Yanga, M.; Yu, J.; Yang, X.; Tian, Y.; Zhang, X.; Zhou, H. *Sens. Actuators, B* **2018**, *272*, 574.
- Mergu, N.; Kim, M.; Son, Y.-A. *Spectrochim. Acta, Part A* **2018**, *188*, 571.
- Zhu, Q.; Li, L.; Mu, L.; Zeng, X.; Redshaw, C.; Wei, G. *J. Photochem. Photobiol., A* **2016**, *328*, 217.
- Sheet, S. K.; Sen, B.; Thounaojam, R.; Aguan, K.; Khatua, S. *J. Photochem. Photobiol., A* **2017**, *332*, 101.
- Shen, Y.; Zhang, X.; Zhang, Y.; Li, H.; Chen, Y. *Sens. Actuators, B* **2018**, *258*, 544.
- Zhu, J.-H.; Wong, K. M.-C. *Sens. Actuators, B* **2018**, *267*, 208.
- Wu, W.-L.; Zhao, X.; Xi, L.-L.; Huang, M.-F.; Zeng, W.-H.; Miao, J.-Y.; Zhao, B.-X. *Anal. Chim. Acta* **2017**, *950*, 178.
- Zhang, L.-J.; Wang, Z.-Y.; Liu, J.-T.; Miao, J.-Y.; Zhao, B.-X. *Sens. Actuators, B* **2017**, *253*, 19.
- Wang, L.; Li, W.; Zhi, W.; Ye, D.; Wang, Y.; Ni, L.; Bao, X. *Dyes Pigm.* **2017**, *147*, 357.
- Kalyanaraman, B.; Hardy, M.; Podsiadly, R.; Cheng, G.; Zielonka, J. *Arch. Biochem. Biophys.* **2017**, *617*, 38.
- Shen, Y.; Zhang, X.; Zhang, Y.; Wu, Y.; Zhang, C.; Chen, Y.; Jin, J.; Li, H. *Sens. Actuators, B* **2018**, *255*, 42.
- Chen, C.; Liu, W.; Xu, C.; Liu, W. *Biosens. Bioelectron.* **2016**, *85*, 46.
- Liu, X.-L.; Niu, L.-Y.; Chen, Y.-Z.; Yang, Y.; Yang, Q.-Z. *Biosens. Bioelectron.* **2017**, *90*, 403.
- Meng, Q.; Ji, H.; Succar, P.; Zhao, L.; Zhang, R.; Duan, C.; Zhang, Z. *Biosens. Bioelectron.* **2015**, *74*, 461.
- Dai, X.; Du, Z.-F.; Wang, L.-H.; Miao, J.-Y.; Zhao, B.-X. *Anal. Chim. Acta* **2016**, *922*, 64.
- Sun, Y.; Shan, Y.; Sun, N.; Li, Z.; Wu, X.; Guan, R.; Cao, D.; Zhao, S.; Zhao, X. *Spectrochim. Acta, Part A* **2018**, *205*, 514.
- Wei, L.-F.; Thirumalaivasan, N.; Liao, Y.-C.; Wu, S.-P. *Spectrochim. Acta, Part A* **2017**, *183*, 204.
- Xie, X.; Yin, C.; Yue, Y.; Huo, F. *Sens. Actuators, B* **2018**, *267*, 76.
- Yang, J.; Yu, Y.; Wang, B.; Jiang, Y. *J. Photochem. Photobiol., A* **2017**, *338*, 178.

About the Authors


Carla Santana Francisco received her bachelor's degree in chemistry in 2006 from Paulista State University, São Paulo, Brazil. She then obtained her master's degree in medicinal chemistry (2009) and her doctorate degree in chemistry (2013) from Minho University, Portugal. Since 2018, she has been a postdoctoral researcher at the Federal University of Espírito Santo (UFES), working first with Professor Dr. Valdemar Lacerda, Jr., and presently with Professor Dr. Álvaro Cunha Neto. Carla's research experience covers a wide range from natural product

chemistry to synthetic and medicinal chemistry, biological assays, molecular modeling, and coumarin synthesis.

Thays Cardoso Valim obtained a B.Sc. degree in forensic investigation and analysis (2013) from the Institute of Technology Sligo, Ireland, and a B.Sc. degree in chemistry (2015) from the Federal University of Espírito Santo (UFES). She received her master's degree in chemistry (2019) from UFES under the supervision of Professor Dr. Alvaro Cunha Neto. Thays has carried out research in analytical chemistry, NMR spectroscopy, food chemistry, forensic science, and environmental chemistry.

Álvaro Cunha Neto received his B.Sc. (1999), M.Sc. (2002), and Ph.D. (2006, with Professor Dr. Gil Valdo José da Silva) degrees in chemistry from the University of São Paulo. He then did postdoctoral research at the State University of

Campinas (2007–2009) under the supervision of Professor Dr. Roberto Rittner Neto. Álvaro is currently Associate Professor at UFES, conducting research in NMR spectroscopy, organic synthesis, and petroleum science.

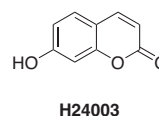
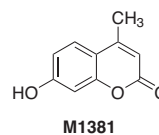
Valdemar Lacerda, Jr., obtained his B.Sc. degree in chemistry in 1997 from the Federal University of Goiás, and received his M.Sc. (2000) and Ph.D. (2004) degrees from the University of São Paulo (USP), conducting research in organic synthesis and NMR spectroscopy. After two years of postdoctoral research at USP, he joined the department of chemistry at the Federal University of Espírito Santo as Associate Professor. His current research interests focus on organic synthesis, NMR studies, theoretical calculations, and petroleum studies. Valdemar is CNPq level 2 researcher, and has published about 80 articles in different high-impact journals. 

PRODUCT HIGHLIGHT

Versatile Building Blocks

Reach new frontiers in your research with our portfolio of coumarins.

Coumarins are an exciting class of compounds with important applications in fluorescence. We currently offer a number of unique coumarins which can be used directly or modified for novel use. Of particular interest are umbelliferone (**H24003**) and 4-methylumbelliferone (**M1381**), which can be derivatized in the 7-position to synthesize a wide variety of chemical probes including some described in the preceding article.



To view these and other new products, visit
SigmaAldrich.com/ActaCoumarins

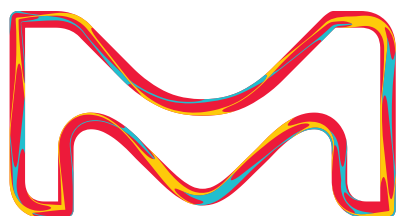
Find your Lead

MERCK

Leverage DNA-encoded library technology for drug discovery

Accelerate your drug discovery with the DNA-encoded library (DEL) technology, an alternative approach to high-throughput screening (HTS) compound libraries for effective hit and lead discovery.

Learn more about the DyNABind off-the-shelf DNA-encoded library, visit SigmaAldrich.com/DEL



The life science business of Merck operates as MilliporeSigma in the U.S. and Canada.

Sigma-Aldrich®
Lab & Production Materials

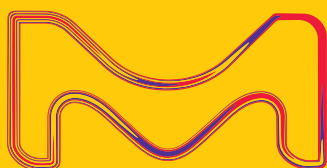
Join the tradition

Subscribe to the *Aldrichimica Acta*, an open access publication for over 50 years.

In print and digital versions, the *Aldrichimica Acta* offers:

- Insightful reviews written by prominent chemists from around the world
- Focused issues ranging from organic synthesis to chemical biology
- International forum for the frontiers of chemical research

To subscribe or view the library of past issues, visit SigmaAldrich.com/Acta



MK_BR3922EN
31869
05/2020

The life science business of Merck operates as MilliporeSigma in the U.S. and Canada.

© 2020 Merck KGaA, Darmstadt, Germany. All Rights Reserved. Merck, Sigma-Aldrich, and the vibrant M are trademarks of Merck. Sigma-Aldrich is a trademark of Sigma-Aldrich Co. LLC, or its affiliates. All other trademarks are the property of their respective owners.